Master's thesis

NTNU
Norwegian University of Science and Technology
Faculty of Natural Sciences
Department of Biotechnology and Food Science

Johanna Tonstad

Adhesion of common salmonid pathogens to Atlantic salmon mucins

Master's thesis in Biotechnology (MBIOT5)

Supervisor: Marit Sletmoen, Karen Dunker

June 2020

NTNU
Norwegian University of
Science and Technology

Johanna Tonstad

Adhesion of common salmonid pathogens to Atlantic salmon mucins

Master's thesis in Biotechnology (MBIOT5)
Supervisor: Marit Sletmoen, Karen Dunker
June 2020

Norwegian University of Science and Technology
Faculty of Natural Sciences
Department of Biotechnology and Food Science

NTNU
Norwegian University of
Science and Technology

Preface and acknowledgements

This thesis marks the completion of the master's degree in Biotechnology (MBIOT5) at the Norwegian University of Science and Technology (NTNU). The work for this project was conducted at the Department of Biotechnology and Food Science (IBT) fall 2019 and spring 2020.

I would like to thank my supervisor, Marit Sletmoen, for all help and feedback regarding experimental results and thesis writing. I would also like to thank my co-supervisor, Karen Dunker, for guidance with the laboratory work, analysis and writing, as well as helping me with the numerous problems experienced with the AFM. The help I have gotten from Swapnil Vilas Bhujbal is also greatly appreciated. Additionally, I am grateful to have been part of the MicroMucus project, surrounded by a group of helpful and talented researchers and students.

My classmates and friends must be thanked for making my time at NTNU a great experience. I would also like to thank my family for the support during the years. Lastly, I would like to thank my friend Maren, for always being there.

Trondheim, June 2018 Johanna Tonstad

Abstract

Fish are covered by mucus on all external epithelial surfaces, constituting the first line of defense against hazardous organisms. For a pathogen to enter and infect the fish, it must first pass through this barrier in the skin, the gut or the gills. Mucins are the major constituent of mucus, and these glycoproteins play various roles in bacterial adhesion. Understanding the properties of these mucins and how they interact with bacteria, is of great importance for the development of different strategies to prevent outbreaks of disease in the aquaculture industry. Nonetheless, the research into the adhesion mechanisms of pathogens to mucosal barriers of fish is limited. The main objective of this study was to investigate the adhesion of the pathogenic bacteria *Aeromonas Salmonicida* and *Yersinia Ruckeri* to Atlantic salmon (*Salmo salar*), to gain knowledge of the adhesion strategies executed by these salmonid pathogens.

The experimental data presented in this thesis was obtained by AFM operated in force spectroscopy mode. This tool enables detection of interactions in the piconewton range and can give an indication of the adhesive strength and the interaction type of a bacteria. Force curves were obtained through AFM measurements, and deadhesion work and rupture forces of interactions between the pathogens and Atlantic salmon skin and gut mucins were determined. Deadhesion work showed that *A. Salmonicida* had relatively little binding with both types of mucins, and that *Y. Ruckeri* bound better to skin than gut mucins. The rupture forces were relatively weak for interactions with both types of bacteria indicating that the bacteria adhere to the mucosal surfaces with weak intermolecular interactions. To investigate the role of sialic acids in adhesion of the pathogens, AFM measurements were executed with the pathogens and mucins treated with neuraminidase. The results from these experiments suggested that *Y. Ruckeri* had sialic acid-specific lectins, whereas adhesion of *A. Salmonicida* is hindered by these terminal residues. Furthermore, measurements were executed with *A. Salmonicida* directly to the skin mucosa of salmon fry, although no interactions were recorded.

Sammendrag

Fisk er dekket av slimhinner, mucus, på alle ytre overflateepitel, som utgjør den første forsvarslinjen mot farlige organismer. Skal et patogen infisere en fisk, må det først passere gjennom denne barrieren i skinnet, tarmen eller gjellene til fisken. Mucin er en av hovedkomponentene i mucus, og dette glykoproteinet har ulike funksjoner i bakteriell adhesjon. I senere tid har det blitt viktig å oppnå en forståelse av egenskapene til mucinene og hvordan de interagerer med bakterier for å utvikle nye strategier for å forhindre sykdomsutbrudd i havbruksnæringen. I dag er denne forskningen på adhesjonsmekanismer mellom patogener og mucusoverflatene til fisk mangelfull. Hovedmålet med denne masteroppgaven var å undersøke og få kunnskap om adhesjonsmekanismene til de patogene bakteriene *Aeromonas Salmonicida* og *Yersinia Ruckeri* på atlanterhavslaks (*Salmo salar*).

Atomkraftmikroskopi (AFM) ble brukt for å samle den eksperimentelle dataen som ble presentert i denne oppgaven. Dette instrumentet kan måle interaksjoner helt ned på piconewton nivå, som kan gi en indikasjon på typen interaksjon som oppstår mellom bakterier og muciner. AFM målinger resulterte i kraftkurver som kunne brukes til å bestemme deadhesjonsarbeid og brytningskrefter for interaksjoner mellom de patogene bakteriene og muciner fra skinnet og tarmen til atlanterhavlaks. Det målte deadhesjonsarbeidet viste at *A. Salmonicida* festet seg lite til begge typer muciner, mens *Y. Ruckeri* festet seg bedre til skinnet enn til tarmen. Brytningskreftene var relativt lave for interaksjoner med begge typer bakterier, som indikerer at bakteriene binder seg til mucusoverflater med svake intermolekylære interaksjoner. For å undersøke rollen til sialinsyrer i adhesjonen til bakteriene ble det gjennomført AFM målinger av bakteriene og muciner behandlet med neuraminidase. Resultatene fra disse eksperimentene indikerte at *Y. Ruckeri* har lektiner som spesifikt kan binde seg til sialinsyre, mens adhesjon av *A. Salmonicida* blir hindret av disse strukturene. I tillegg ble adhesjonen av *A. Salmonicida* direkte til skinnet på lakseyngel målt, men ingen interaksjoner ble målt.

Table of Contents

Abbreviations

AFM	Atomic force microscopy
Cys	Cysteine
CRD	Carbohydrate-recognition domain
EDC	N-(3-dimethylaminopropyl)-N'-ethylcarbodiimide hydrochloride
ERM	Enteric redmouth disease
Gal	Galactose
GalNAc	*N*-Actylgalactosamine
GALT	Gut-associated lymphoid tissue
GIALT	Gill-associated lymphoid tissue
GlcNAc	*N*-acetylglucosamine
GuHCl	guanidine hydrochloride
Kdn	2-keto-deoxynonulosonic acid
MALT	Mucosa-associated lymphoid tissue
MQ	Milli-Q
MUB	Mucus-binding
Neu	Neuraminic acid
Neu5Ac	5-*N*-acetylneuraminic acid
Neu5Gc	5-*N*-glycolylneuraminic acid
NeuT	Neuraminidase treated
PBS	Phosphate buffered saline
SALT	Skin-associated lymphoid tissue
SCFS	Single-cell force spectroscopy
Ser	Serine
SGM	Salmon Gnotobiotic Media
SMFS	Single-molecule force spectroscopy
STP	Serine - Threonine - Proline
Thr	Threonine
TSA	Tryptic soy agar
TSB	Tryptic soy broth
VNTR	Variable number tandem repeats

List of Figures

List of Tables

Introduction

Fish constitute a major source of protein, fatty acids, vitamins, minerals and essential micronutrients for an increasing portion of the world's population. Consequently, the aquaculture industry is the fastest growing food-producing sector, and provides around 50% of the fish that is consumed in the world today [1]. Atlantic salmon is one of the main cultivated species, and is an important part of the expanding aquaculture industry, with Norway as the main producer. Disease outbreaks are a major concern for the expansion of aquaculture, and it leads to significant economic losses every year [2, 1]. Furunculosis and Enteric redmouth disease, caused by *A. Salmonicida* and *Y. Ruckeri*, are two of the most harmful diseases of salmonids, causing severe economic impacts on the industry [3, 4].

Even though vaccines are effective in preventing diseases in aquaculture, the possible side effects can significantly reduce the health and welfare of the fish [5]. Furthermore, vaccinations are often expensive and have limited effect on certain pathogens [6, 4]. In addition to vaccinations, antibiotics are used to fight infections. However, this adds to the spreading of antibiotic resistant bacteria and genes into our environment which is highly disadvantageous [6]. Development of antibiotic resistance have been reported in *A. Salmonicida* and *Y. Ruckeri*. Such findings, and the interest in increasing fish welfare and aquaculture productivity, highlights the need for alternative treatments for diseases in aquaculture [7, 5].

To produce alternative treatments for diseases in aquaculture, an improved understanding of host-pathogen interactions are necessary [6]. Fish are covered by mucus on all epithelial surfaces facing the external environment, which constitutes the first line of

defense against the pathogens [8]. For the pathogen to enter and infect the host, it must pass this barrier in the skin, the gut or the gills [9]. Mucins are the major constituent of mucus, and it has been suggested that these glycoproteins are an important factor in understanding bacterial adhesion interactions [10]. A prominent method for studying molecular interactions is force spectroscopy. This atomic force microscopy (AFM) based approach allows for detection of interactions in the piconewton range and can give an indication of the adhesive strength and the interaction type of a bacteria [11]. Using this approach to measure interactions between pathogens and mucins can unveil important knowledge of the mechanical processes that occur during bacterial adhesion, and uncover potential routes of entry into the host. This could provide valuable information for the production of potential treatments.

1.1 Bacterial adhesion

Adhesion is an important part of the bacterial life style. Bacteria can adhere to all surfaces, to each other and to other cells. Adhesion to eukaryotic cells can serve various purposes in commensalism, symbiosis and pathogenesis, providing survival for the microbe [12]. As bacterial adhesion is a prerequisite for infection of host tissues, this mechanism is quite important in the understanding of pathogenesis and how to prevent it [13]. Even so, for many bacteria the mechanisms for adhesion are not well known [10].

Bacterial adhesion involves a complex interplay of forces that can be either specific (receptor-ligand interactions) or nonspecific (hydrophobic and electrostatic interactions) [14]. In most cases, bacteria adhere directly to host cells by adhesins binding specifically to host cell receptors. These interactions have a given strength, presumably optimized to enable strong binding to the substrate, whilst also being weak enough for the bacteria to detach and migrate to other locations. As mucosal surfaces cover several of the entry routes into the host, binding to these areas are essential, especially binding to the

glycoprotein mucin. Consequently microbes have evolved adhesion mechanisms specific to the oligosaccharide motifs of the glycoproteins, by glycan-lectin or glycan-glycan binding [10, 15]. A simplified illustration of these specific interactions are shown in figure 1.1.

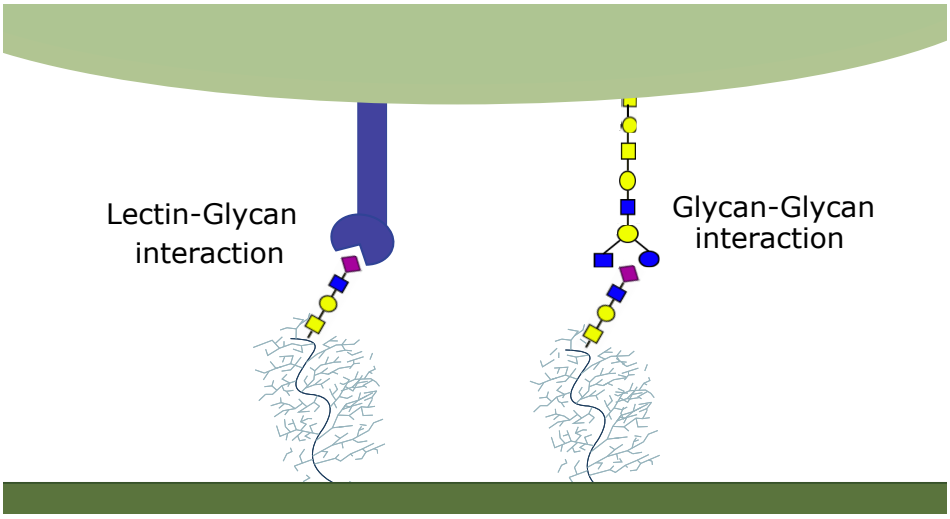

Figure 1.1: Illustration of specific interactions, lectin-glycan and glycan-glycan interactions, involved in bacterial adhesion to host surfaces.

1.1.1 Pili-based adhesion to mucosal surfaces

The most studied mechanism is adhesion via bacterial lectins, called adhesins, and their corresponding glycosylated receptors [15]. Adhesins occur commonly as elongated, multisubunit protein appendages, known as pili or fimbriae. The carbohydrate-recognition domain (CRD) is found in a minor subunit located at the tip of the pili. This site facilitate binding to glycans, either on terminal sugar residues or to internal sequences in the oligosaccharide chain. The affinity of these adhesin-receptor bonds are generally low. However, frequent clustering of receptors and adhesins allow multiple bonds to be formed simultaneously, thus increasing the binding strength [16].

The CRDs have subtle molecular complementarity that allows interaction only with their correct carbohydrate cognate, leading to a high specificity in these interactions [17]. This specificity can be illustrated by the bacteria *Escherichia coli* and its ability

to bind to glycolipids with Neu5Gc, but not with Neu5Ac, which differs only with a single hydroxyl group present on Neu5Gc. Most bacteria have multiple adhesins with diverse carbohydrate specificity, defining the preferred microenvironmental niche of each bacterial strain [16].

Pilins are the other major subunits of the pili, organized in a helix-like arrangement in the form of a rod. These structures are able to elongate by an unfolding process caused by shear force, and can retract back to its original structure with the absence of this force, shown in figure 1.2. This is important for the ability of bacteria to withstand high shear forces originating from rinsing flows [13, 18].

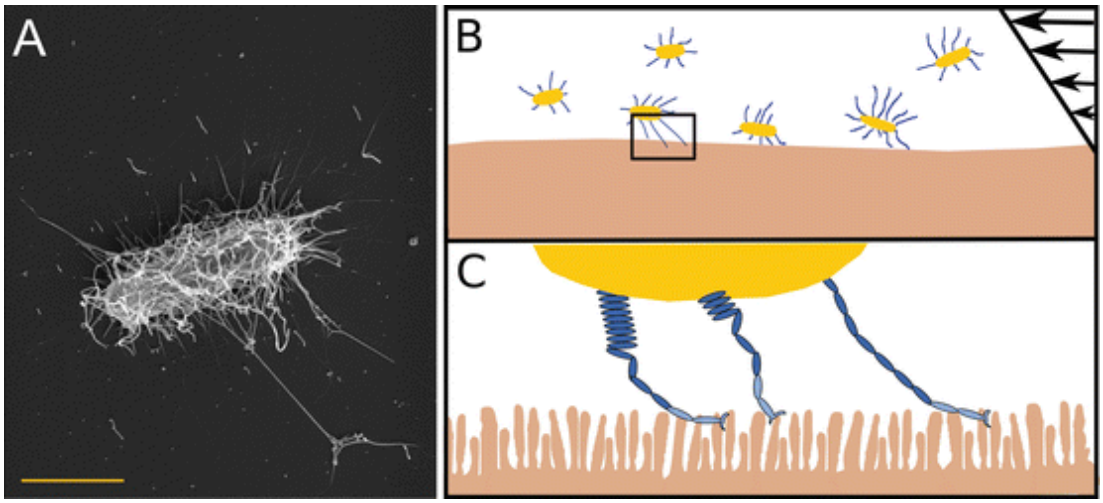

Figure 1.2: Model of bacteria attaching to intestinal epithelium via pili. (a) Scanning Electron Microscopy micrograph of an E. coli expressing multiple adhesion pili. Magnification bar is 1.0 µm. (b) Illustration of bacteria close to the intestinal epithelium and exposed to a gradient flow. (c) Bacteria attached to microvilli via pili that are partially uncoiled (left and middle) or completely uncoiled (right). Obtained from [18].

1.1.2 Non pili-based adhesion to mucosal surfaces

Some bacteria express proteins that specifically recognize mucins. Various mucus-binding (MUB) proteins have been found, but they are mainly described in lactic acid bacteria. This protein have domains that are similar to mucin-binding protein (MucBP), which is a domain found in a variety of bacterial proteins known for their

ability to adhere to mucins. MUB also has similarities with pathogenic gram-positive adhesins which bind specifically to sialic acids of glycoproteins [19, 20].

1.1.3 Glycan-glycan interactions

Bacterial cells are covered by various glycans, such as lipopolysaccharides and lipo-oligosaccharides, which play a role in attachment to glycans on host surfaces. These types of interactions have mostly been characterized as low-affinity, weak interactions, although some studies have demonstrated that high-affinity binding occurs. It has also been shown that these types of interactions are critical for the pathogenesis of some bacteria [21, 10].

1.2 Mucus

Mucus is a viscoelastic semi-adherent secretion covering mucosal surfaces. The majority of viruses, bacteria, yeast, protozoa and multicellular parasites enter their hosts via these mucosal surfaces, and mucus constitutes the first line of defense between the external environment and the host. The second line of defense is the epithelial glycocalyx, which is partially integrated with the overlying gel [15, 22]. The major macromolecular component of mucus are mucin glycoproteins. Additional constituents include water, electrolytes, lipids and various proteins, which together make up a relatively impervious gel that acts as a lubricant, a barrier for pathogens and a permeable layer for the exchange of gases and nutrients with the underlying epithelium [23, 24].

Mucins, with its high carbohydrate content, are responsible for several of the physiochemical properties of mucus. Expression of different types of mucins, variations in mucin glycosylation and the co-secretion of mucin-associated molecules creates a responsive system that can be adapted to local physiological requirements. Consequently, the nature of mucus varies between different locations, and are influenced by changes to the sub- and supra-mucosal environment, such as hormonal status,

inflammation and microbial colonization [22]. The mucus layer is not static, but constantly renewed. This enables the mucus to clear trapped materials, and rapidly adjust to the changes in the environment [15].

1.2.1 Mucins

Glycoproteins are carbohydrate-protein conjugates where proteins are covalently linked with one or several oligosaccharides of varying complexity. Mucins are secreted or membrane-bound glycoproteins with a high level of O-linked oligosaccharides [17, ch. 7]. This glycoprotein contribute to the mucoadhesive and viscoelastic nature of mucus [25]. Microbial interactions with epithelial surfaces are attributed to mucins and its ability to present ligands to block microbial binding or stabilize colonization. In this way, mucus is able to allow colonization of commensal bacteria, whilst being a barrier for pathogenic bacteria [22].

1.2.2 Mucin structure

The mucins family includes over 20 MUC genes, that share many common features [26]. The dense array of O-linked carbohydrates comprise over 80% of the mucin's mass, ranging from 0.5 to 20 MDa. The carbohydrates are primarily *N*-acetylgalactosamine (GalNAc), *N*-acetylglucosamine (GlcNAc), fucose, galactose (Gal), sialic acids, mannose and sulfate [23]. The O-glycosidic linkage is formed through GalNAc, which links to the hydroxyl side chain of serine (Ser) and threonine (Thr) on the protein core. The size, charge and branching of the glycans varies between different mucosal regions [22].

The protein core is arranged into two broadly distinct regions and make up the remaining 20% of the mucin mass. One region is the centrally located variable number tandem repeats (VNTR) which is unique to each MUC gene. This segment is rich in Ser, Thr and proline (STP) and serve to carry the glycan chains [23]. 100s of complex oligosaccharide structures can be bound to this part, forming a filamentous protein with a "bottle-brush" appearance [15]. The second type of region is located at the amino and

carboxy terminals and sometimes scattered between the STP-repeats. Unlike the STP-region, which varies for each MUC species, this region share a large degree of similarity between the species. It is characterized by a high proportion of cysteine (Cys), low amounts of Ser and Thr and very little O-glycosylation. The amino acid sequence and structures of these Cys-rich domains contribute to intra- and intermoleuclar disulphide bonds [15, 23, 24].

1.2.3 Secreted and membrane-bound mucins

Secreted mucins and membrane-bound mucins are the main types of mucins. The secretory mucins can be further subclassified as gel-forming mucins and non-gel-forming mucins. Gel-forming mucins are the major constituent of mucus and contribute to its viscoelastic properties due to their ability to cross-link creating extended mucin networks. The secreted non-gel-forming mucins are able to self-aggregate, but does not seem to contribute significantly to mucus properties. Secreted mucins have D-domains similar to von Willebrand factor D (vWF-D) and Cys-rich domains located at the amino end, and Cys-rich domains at the carboxy terminal, shown in figure 1.3 [15, 26].

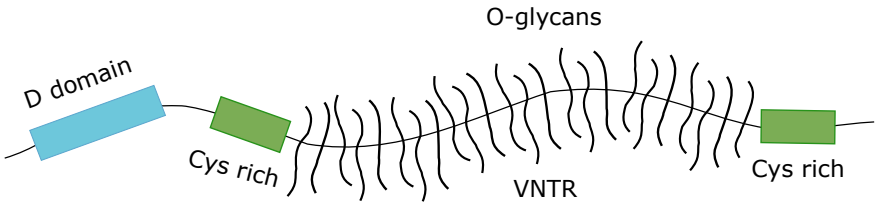

Figure 1.3: Simplified model of a large secreted mucin. The glycoprotein contains a D domain, two cys rich regions and a VNTR region.

Membrane-bound mucins are present on the apical membrane of all mucosal epithelial cells, and are a prominent part of the glycocalyx. The extracellular domain primarily consist of VNTR, creating rigid elongated structures that provides a barrier that limits access and interacts with cells on the surface. The cytoplasmic domains of cell-bound mucins appears to interact with signaling molecules allowing them to be involved

in signaling pathways in response to microbes or toxins. A simplified model of a membrane-bound mucin is shown in figure 1.4. The membrane-bound mucins may be shed into the overlying mucus, and can therefore also be seen as components of secreted mucus [15, 25].

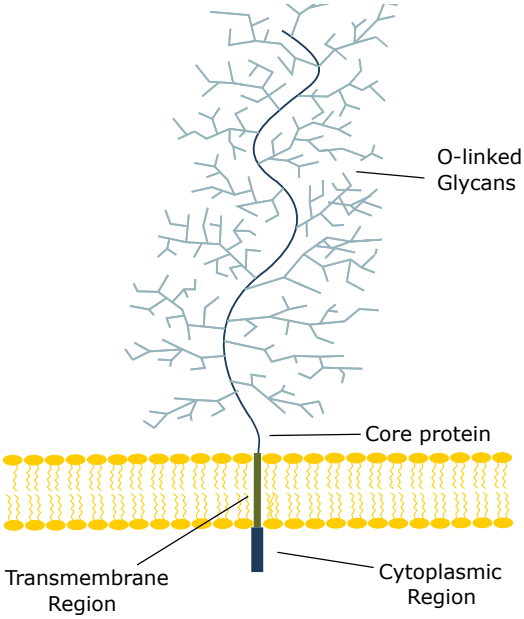

Figure 1.4: Simplified model of membrane-bound mucin. The glycoprotein consist of a cytoplasmic region, a transmembrane region and a core protein with O-linked glycans attached.

1.2.4 Mucin O-glycans

Mucins contain hundreds of heterogenous O-glycans attached to the protein core. The functions of these glycans are many. The extensive O-glycosylation on mucins leads to an elongated rod-like conformation, and can protect the core from proteolytic enzymes. O-glycans are hydrophilic and often negatively charged, giving them the ability to bind water and salts contributing to its viscous and adhesive properties. Many of the terminal sugars may function as a ligand for lectins, or mask underlying ligands [27, 15].

Mucin properties are controlled by the great variety, density and clustering of their glycans. This content varies according to cell lineage, tissue location and developmental

stage. Glycosylation can also be altered in response to environmental factors such as mucosal infection and inflammation [15, 27].

GalNAc O-linked to Ser/Thr is the initiating sugar of the mucin glycans [27]. The addition of monosaccharides to different positions on the GalNAc yields a group of eight different core structures, whereas structures 1-4 are most common. Each core is elongated by a stepwise addition of monosaccharides with glcyosyltransferases, yielding linear or branched O-glycans. The specific structures formed are determined by the expression of specific glycosyl transferases, resulting in glycosylation being regulated by genetics, tissue-specific enzyme expression and host and environmental factors [26, 24, 15]. The carbohydrate chains are commonly terminated by fucose, sialic acids, Gal, GalNAc, GlcNAc and sulphate. Many of these terminal sugar are antigenic or can be recognized by lectins. Sialic acids and sulfates adds negative charges to the mucin oligosaccharides [24, 27].

1.3 Sialic acids

Sialic acids are structurally diverse nine-carbon ketosugars. These sugars can be found at the terminal end of glycoproteins and have several functional roles [28, 29]. Common to all sialic acids is the carboxylate at the 1-carbon position, which is usually ionized at physiological pH. The structure, negative charge and terminal position give sialic acids a crucial role in cell-cell and cell-moleucle interactions, with potential to act as inhibitors or be essential components of recognition molecules. Moreover, sialic acids present a source of potential carbon, nitrogen and cell wall metabolites necessary for bacterial growth and survival [30].

The most common sialic acid is 5-*N*-acetylneuraminic acid (Neu5Ac), composed of a nine-carbon backone, with a carboxylate group at C-1, an acetamido group at the C-5, and a glycerol tail composed of carbons 7-9 [28]. The sialic acid family consists of related structures that vary at the C-5 carbon, including 5-*N*-glycolylneuraminic acid

(Neu5Gc), 2-keto-deoxynonulosonic acid (Kdn) and neuraminic acid (Neu), shown in figure 1.5 [29].

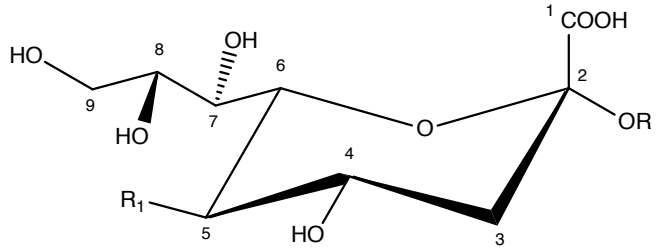

Neu5Ac: R_1 = NH-CO-CH_3 Neu: $R_1 = NH_2$

Neu5Gc: R_1 = NH-CO-CH_2-OH Kdn: R_1 = OH

Figure 1.5: The structure of the core sialic acids, Neu5Ac, Neu5Gc, Neu and Kdn. The sialic acids share a backbone and a glycerol-like side chain. Variations in the C-5 carbon, yield different core structures. Various modifications may occur to the molecules, including attachment of chemical groups to the hydroxylgroups on C-4, C-7, C-8 and C-9 carbons.

The position of the carboxylate groups make the sialic acids strong acids, and the glycerol side chain provides opportunities for hydrogen binding. The N-acetylgroup on Neu5Ac promotes hydrophobic interactions, while the N-glycolylgroup of Neu5Gc promote hydrophilic interactions. Each of the moieties of sialic acids participate in the binding specificites and functions of mucins, creating diversity amongst the family of acidic sugars. A second level of diversity comes from various modifications to the sialic acids. Different chemical groups, such as O-acetyl, can be attached to the hydroxyl groups of C-4, C-7, C-8 and C-9 [29]. Moreover, terminal sialic acids can form different glcyosidic linkages to underlying carbohydrates, through an α-glycosidic bond between the C-2 hydoxyl of the sialic acid to various positions of the carbohydrate [28].

The structure and position of sialic acids make them important in the protective functions of mucins. Their size and negative charge enable them to function as a protective shield for the subterminal part of the molecule. Steric repulsion between oligosaccharide chains caused by charge, contributes to the mucins extended rod-like

conformation. This structure prevents proteolytic degradation [31]. Providing the mucus with a high anionic charge and an aptness to bind water, the sialic acids contributes to the hydrating and protective features of the barrier [29]. As terminal residues of mucins, sialic acids can mask the underlying sugars preventing recognition of possible binding sites from bacterial lectins, thus aiding the protective properties of mucus [32]. Due to cell surfaces being abundant with sialic acids, it is not surprising that pathogenic bacteria have evolved mechanism to target these molecules. The diverse sialic acids can function as a barrier, as well as a facilitator of binding for microbes. This complexity is thought to be the result of an ongoing "arms race" between animals and microbial pathogens [29].

1.3.1 Sialidase

Sialidases, or neuraminidases, are sialic acid-releasing exoglycosidases that catalyze the removal of sialic acids linked to oligosaccharide chains [33]. Sialidase exist in vertbrates and in a variety of microbes, viruses and parasites [34, 35]. Bacterial sialidases contribute to the host-microbe interactions, and can be used to promote bacterial survival in mucosal environments. Their enzymatic activity can unmask underlying ligands to which bacteria or their toxins adhere. Furhtermore, these terminal sialic acids and their subterminal carbohydrates can be utilized as a nutritional source [35]. The enzymes play a role in pathogenesis, as well as being a common factor in the carbohydrate catabolism of many nonpathogenic species. They do not exert direct toxic effects, but pathogens can use it to damage cells by releasing a massive amount, in addition to toxic factors [31]. Sialidase activity can be slowed down or inhibited by modifications to the sialic acid [35].

1.4 Model organisms

1.4.1 Atlantic salmon

Atlantic salmon is an anadromous fish species belonging to the diverse group of ray-finned fishes called Teleostei [36]. More than 2000 genetically distinct populations are found around the North Atlantic Ocean. After hatching, juveniles typically spend 1-5 years in the rivers before migrating to the sea. Atlantic salmon fry utilize their yolk sac as their primary source of energy the two first months after hatching. Long-distance migrations between freshwater and ocean habitats expose Atlantic salmon to various threats, and many anthropogenic factors have contributed to the decline of Atlantic salmon over the years [37]. Today, around 99% of Atlantic salmon are found in farms, not in the wild [38].

The adult teleost fish is covered by mucus on all epithelial surfaces facing the external environment [8]. These mucosal surfaces are an important part of the immune system as it constitutes the first line of defence against the outer infectous agents, and contains a variety of leukocytes to respond to antigens encountered in these areas. The main mucosa-associated lymphoid tissues (MALT) of teleost are the skin-associated lymphoid tissue (SALT), the gut-associated lymphoid tissue (GALT), the gill-associated lymphoid tissue (GIALT) and the recently discovered, less known nasopharynx-associated lymphoid tissue (NALT) [9, 36], shown in figure 1.6.

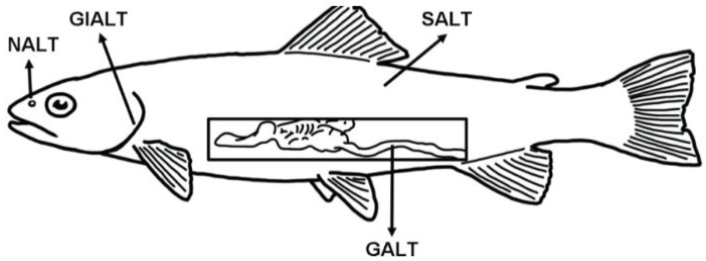

Figure 1.6: Illustration of the four teleost main mucosa-associated lymphoid tissues (MALT) and their anatomical localization. GALT: gut-associated lymphoid tissue; SALT: skin-associated lymphoid tissue; GIALT: gill-associated lymphoid tissue; NALT: nasopharynx-associated lymphoid tissue. Obtained from [9]

Fish skin is one of the largest barriers to the exterior environment, and plays a crucial role in protection against pathogens as well as numerous other biological processes such as osmoregulation and ion exchange [39]. An important protective function of the skin mucosa is its ability to secrete and replace the mucus in a high rate, enabling it to trap and immobilize bacteria which is subsequently removed by the water currents. Additionally, the skin has an underlying layer of mucus adjacent to the epithelia with the ability to remain unstirred despite the vigorous shearing actions of the water currents [36].

Atlantic salmon mucins

Knowledge of the mucin O-glycosylation in fish is very limited compared to mammalian mucins. However, some advances have been made the recent years, shedding light on the structure, O-glycosylation and sialylation of mucins from Atlantic salmon [8].

A study from Micallef *et al.* used next-generation sequencing of Atlantic salmon skin, revealing partial mucin sequences with homology to the human MUC2, MUC5A and MUC5B mucins [39]. These belong to the group of gel-forming mucins and are major constituents of the mucus-gel. The viscoelastic properties of the mucus is attributed to these mucins due to their ability to cross-link and form extended mucin networks [15].

Mucin O-glycosylation of Atlantic salmon were investigated by Jin et al. Mucins from the skin, pyloric ceca and proximal and distal intestine were characterized using mass spectrometry. From the five Atlantic salmon examined, 109 O-glycans were found. The study showed that the O-glycan profile differs depending on tissue. Skin O-glycans were shorter and less diverse (2-6 resiudes, 33 structures) than intenstinal glycans (2-13 residues, 93 structures). Skin mucins carried O-glycan cores 1, 2, 3 and 5, and had sialyl-Tn as the most predominant structure. Intestinal mucins carried cores 1, 2 and 5, and sialylated core 5 was the most dominant structure. Three types of sialic acids (Neu5Ac, Neu5Gc and Kdn) were found in the skin mucins, where Neu5Ac was the most dominent one. The gut mucins only contained Neu5Ac [8]. Further studies by

Padra et al. showed that the intestinal mucins contained a higher amount of sialic acids than skin mucins [40]. Another study by Padra and coworkers showed that skin mucins were predominantely linear, while the intestinal were mostly branched [5].

1.4.2 *Aeromonas Salmonicida*

A. Salmonicida is a gram-negative, facultative anaerobic, non-motile and rod-shaped Aeromonadaceae and is the causative agent of furunculosis in salmonids [5, 41]. Furunculosis is a systemic disease characterized by high mortality and high morbidity, which occurs in both wild and farmed Atlantic salmon in addition to other salmonid species. The disease is very common worldwide, and spreads through contact with infected fish or by exposure to water contaminated with *A. Salmonicida* [4].

All species of the Aeromonas genus are motile, except for *A. Salmonicida* [42]. This bacteria does not contain flagella, but two functional types of the adhesive type IV pilus (Tap and Flp) and type I (Fim) complexes has been found. Studies have shown that in spite of their known adhesive capabilities these proteins are not the major virulence factors for *A. Salmoninicida*, although they are not redundant [43, 44]. The most well studied *A. Salmonicida* adhesin is the surface layer, S-layer, sometimes referred to as the A-layer, which contains lipopolysaccharides. This layer is nonspecific, but important for adherence due to its hydrophobic nature [42].

Despite of *A. Salmonicida* being one of the most important salmonid pathogens, with a big impact on the aquaculture industry, the adhesion mechanism of the bacterium is not fully understood. The route of entry may be through the mucosal surfaces of skin, gut or gill [45]. It has been suggested that *A. Salmonicida* gain entry to the host by damaging the intestinal lining, facilitated by the release of toxins [46, 42]. Padra et al. showed that *A. Salmonicida* bound better to intestinal mucins than skin mucins [40], and that intestinal mucins enhanced growth for the bacterium, whereas the skin O-glycans do not [5]. These studies also demonstrated that sialic acids has a complex role in relation to *A. Salmonicida*. It was suggested that Neu5Ac promotes adhesion

between mucins and *A. Salmonicida*, whilst also protecting the growth-enhancing O-glycans underneath the terminal Neu5Ac from *A. Salmonicida* access [40, 5].

1.4.3 *Yersinia Ruckeri*

Y. Ruckeri is a gram-negative rod-shaped enterobacterium, and is the causative agent of yersiniosis or enteric redmouth disease (ERM) in fish [3]. Typical features of the infection include hemorrhages of the mouth or tongue, darkening of the skin and inflammation of the gut [47]. The bacterium is widely spread in fish populations throughout North and South America, Europe, Australia, South Africa, the Middle East and China [1]. Although several fish species are susceptible to this agent, salmonids and rainbow trout are most commonly targeted [3].

The *Y. Ruckeri* bacillus is approximately 0.75 µm in diameter and between 1.0-3.0 µm in length. The bacterium does not possess a capsule, but flagella is common for several strains of the bacteria resulting in various motility for the different strains [3]. Hightroughput DNA sequencing of *Yersinia* species verified that *Y. Ruckeri* share the same core set of genes with the other members of the genus [48].

Despite the importance of *Y. Ruckeri*, little is known about the pathogenic mechanisms the bacteria use to overcome host defenses and cause disease. Coquet et al. isolated a strain that was able to form biofilms on solid supports, which suggested a high adhesion efficiency possibly caused by the expression of flagella or pili [49, 3]. Two types of genes for adhesins have been identified and characterized for *Y. Ruckeri*, namely *Y. Ruckeri* invasin, and *Y. Ruckeri* invasin-like molecule, although the function of these molecules is not yet fully understood [47]. Histological examination of rainbow trout infected with *Y. Ruckeri* indicated that gills are an important entryway for the pathogen, from which it spreads to other organs [50]. Another study performed by Tobback et al. indicated that gut and gills are both important in the initial interactions with *Y. Ruckeri* to its host [51]. The effect of sialic acid for *Y. Ruckeri* binding is not known, although genes for sialic acid catabolism have been found for 9 *Yersinia* species, allowing the possibility

for *Y. Ruckeri* to contain the same set of genes [52].

1.5 Atomic force microscopy

Atomic force microscopy (AFM) is a three-dimensional topographic technique for imaging surfaces of objects at nanometer scale resolutions. AFM is a type of scanning probe microscope, which is based on the interaction between a sharp tip and the atoms of the sample surface [53]. This makes it different from other microscopic techniques, as it physically "feels" the sample's surface to build a topographic map based on the height of the surface, instead of forming an image by focusing light or electrons on the surface. As well as its use as a microscope, developments have rendered it possible to measure forces between samples and to manipulate or modify sample surfaces [54]. The AFM can therefore be divided into three major application areas: imaging, force measurement and manipulation [11].

Since its invention in 1986, the major applications of AFM have been within visualization of microcircuits, material sciences and nanotechnology. However, in recent years application of AFM to biological and biomedical research has increased exponentially. Utilization of this instrument provides several important advantages in studies of biological samples. AFM experiments does not require sample preparation such as freezing, metal coating, vacuum or dye, thus preserving the biological functions of the samples. Additionally, the AFM is capable of operating in air and in fluids, allowing measurements to be obtained at near-physiological conditions [55, 56].

1.5.1 AFM instrumentation

The main components of an AFM are the microscope, control electronics and a computer. The microscope itself is where the scanning of the sample surface or other types of force measurements take place. Microscope components include a cantilever, a piezo scanner, a laser diode and a position sensitive detector, shown in figure 1.7. The piezo

scanner is used for controlling the movement of the probe, enabling measurement of very small movements [54]. The laser diode emit laser towards the tip of the cantilever, which is reflected towards a position-sensitive photodiode. Interactions between the tip and the sample leads to bending of the cantilever, allowing the photodiode to record displacements of the laser beam.

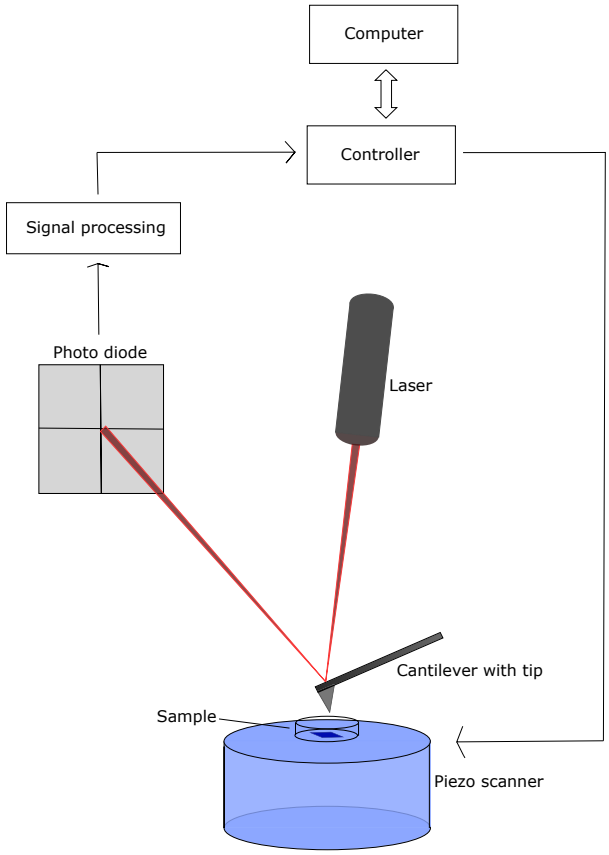

Figure 1.7: The basic principle of an atomic force microscope. The surface of the sample is scanned by the cantilever, which bends when it encounters force. Laser is emitted from the laser diode onto the tip of the cantilever, and reflected to the photo diode. The feedback loop is implemented in the controller. The computer is used to setup parameters for the controllers and collect data.

The relationship between cantilever deflection and force is give by Hooke's law

$$F_d = -k\Delta z \tag{1.1}$$

where F is the force, k is the spring constant and Δz is the deflection distance.

Information obtained from the deflection can be used to create topographic maps or obtain information of the physical properties [11, 55]. The feedback loop is implemented in the controller, managing signals between the cantilever and the piezo, to the keep the force between the tip and sample constant [54].

The AFM cantilever is used as a sensor to detect the probe-sample interaction. These cantilevers commonly consist of a sharp tip and a micro cantilever, although other types are common, such as colloidal and tipless cantilevers. The cantilevers are usually made of silicon or silicon nitride and are often coated with another material. The size of the micro cantilever vary from 30-40 μm in width and 125-450 μm in length. The thickness ranges from a fraction of an μm to a few μ. Variations within these properties, in addition to the various types of tips produced, provides a wide range of cantilevers with the ability to measure forces ranging from a few pN to hundreds of nN, fit for different types of measurements [11].

1.5.2 Force spectroscopy

One of the major application areas of the AFM is force spectroscopy. The purpose of this measurement is detecting the force between the tip and the sample surface [11]. Force spectroscopy keeps the xy position of the AFM probe fixed, while moving it in the z-axis. Force-distance curves are obtained by recording the cantilever deflection in the z position. With highly flexible cantilevers and a high deflection sensitivity, force spectroscopy measurement are able to record interactions with a force down to few pN, thus able to detect single-molecule interactions [57].

Force-distance curves are obtained by approaching the sample with the cantilever and then retracting it, measuring the attractive and repulsive interactions occurring during this process, by Hooke's law. A simplified force-distance curve is shown in figure 1.8, where the force is plotted against distance. As the cantilever approaches the surface attractive forces, usually Van der Waals, overcome the spring constant and the tip jumps into contact with the surface. This is followed by repulsive forces as the cantilever

is driven further towards the sample. When the tip is retracted, initial short range repulsion is overcome by attractive forces driven by the adhesion between the tip and the sample. The interaction is broken when a given force, larger than the adhesion interaction is applied to the cantilever [54, 11].

The approach curve can be used to give quantitative information about the sample's height or mechanical properties, while the retract curve contain information related to the adhesive forces acting between the AFM tip and the surface of the sample [10, 54]. The depth of the negative peak on the retraction curve is a measure of the rupture force required to pull the tip free of the surface. The area enclosed by this peak defines the work executed to break the adhesive interaction [57].

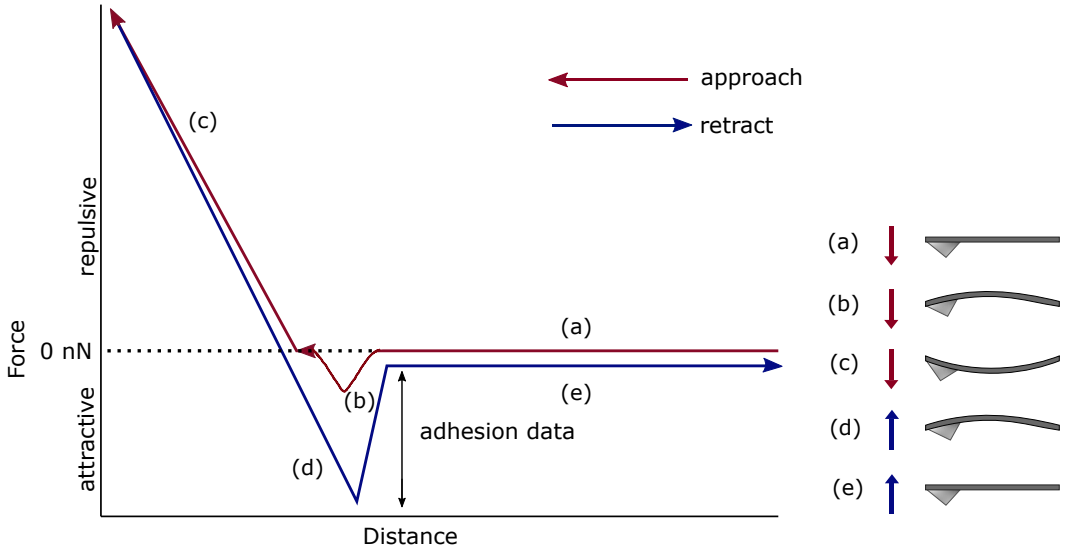

Figure 1.8: Illustration of an AFM force-distance curve. Measurements of the cantilever deflection are made as the tip approaches (a to c) and retracts (d to e) from the sample surface. As the tip approaches initially the forces are too small to give a measurable deflection in the cantilever (a). At some distance the sum of attractive force are larger than the cantilever spring constant and repulsive forces, the tip jumps into contact with the surface (b). The force becomes repulsive as the probe continues to be directed towards the surface (c). At a user-defined point the cantilever is retracted. If adhesion has occurred, the cantilever is pulled towards the surface by the attractive forces (d), until the force applied to the cantilever overcomes tip-sample adhesion (e).

To obtain accurate results, two parameters need to be calibrated, the cantilever deflection sensitivity and spring constant. Deflection sensitivity measures how many nm in

cantilever deflection that corresponds to 1 V in the position sensitive photodiode output. This value depends on the cantilever length and the position of the laser. The spring constant represents the cantilever stiffness. It varies from the thickness, width and length of the cantilever. The precise value of cantilever thickness is usually not known, variations occur during the manufacturing process or as a result of functionalization. The precise spring constant can be calculated by the AFM after obtaining the cantilever sensitivity, by a process called thermal noise method [11, 58].

1.5.3 Force spectroscopy with living cells

Advances in AFM techniques have rendered it possible to measure cell-cell and cell-substrate adhesion. By attaching multiple cells, single cells or molecules to an AFM probe, interaction forces between the cell or molecule and a target surface can be measured. This has lead to advances in our knowledge of the forces driving cell adhesion [59].

Two prominent AFM modes for biological interactions are single-molecule force spectroscopy (SMFS) and single-cell force spectroscopy (SCFS). In SMFS a single molecule, usually a biomolecule, is attached to an AFM tip and specific interactions such as single receptor-ligand bonds or the unfolding mechanism of single proteins, can be measured. SCFS has a living cell immobilized to the tip, allowing measurements of single-cell adhesion forces [60]. These techniques have been used to understand the complex molecular dynamics involved in bacterial attachment, by characterizing and quantifying forces driving adhesion of bacteria [10].

Recent years, studies have provided insight uncovering the binding mechanism of microbial adhesins, bacterial pili, cell-cell co-adhesion. Representative force curves obtained from such studies are shown in figure 1.9, which can give data of adhesion and binding force of mechanical properties [11, 59]. AFM is also useful to gain valuable knowledge about specific bacteria-substrate attachment, including bacteria-glycan adhesions. The binding properties of pili, MUB and other adhesins to glycan structures provide valuable

information which can be used to study the mechanism of different bacteria to mucosal surfaces [10].

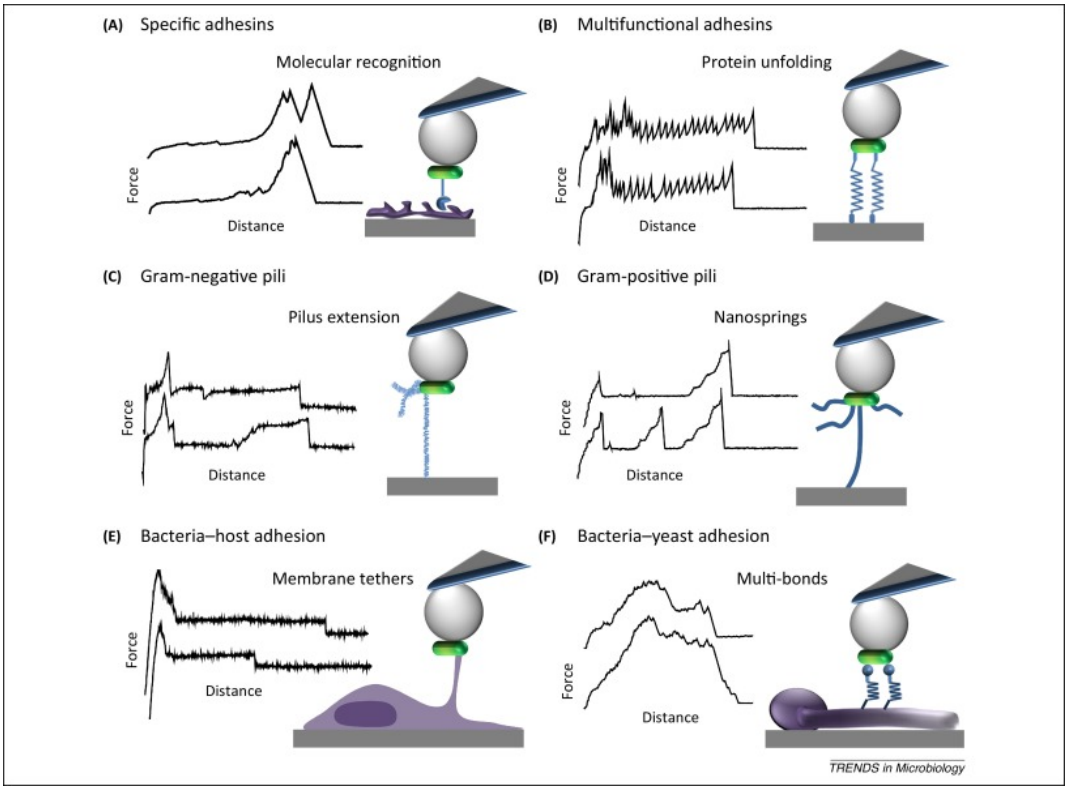

Figure 1.9: Cell adhesion components display a variety of mechanical properties that are important for cell surface interaction. (A) Ligand binding of specific adhesins. (B) Protein unfolding of multipurpose adhesins. (C) Elongation of Gram-negative pili. (D) Spring behavior of Gram-positive pili. (E) Membrane tethers in microbe–host interactions. (F) Multiple macromolecular bonds in bacterium–yeast co-adhesion. Obtained from [59].

Using appropriate procedures for functionalizing AFM probes with molecules or cells is an essential step for measuring molecular interactions. A suitable protocol should include the following: (i) the forces which attach the molecules to the cantilever should be stronger than the intermolecular forces studied; (ii) the attached molecules or cells should be intact and have enough mobility to interact with the substrate; (iii) and for SMFS and SCFS the number of cells should be carefully monitored [60, 59]. Over the past 20 years, various protocols have been developed, originating from Razatos and coworkers procedure for immobilization of *E. Coli* with polyethylenimine (PEI) [61,

10]. This strategy includes using electrostatic interactions between the functionalized, positively charged cantilever and the negatively charged bacterial surface polymers. PEI and poly-(L-lysine) (PLL) are used for this purpose, although recent studies have shown possible antimicrobial effects with these molecules [62]. The wet adhesive polydopamine (PDA) has been used to establish covalent bonds between bacteria and cantilever, providing strong stable interactions. Chemicals containing amino-groups, such as silanes, have been used to establish bonds with the negatively charged carboxyl group present on the bacterial surface. The great variety between bacteria present challenges in finding one immobilization method that works for all [62]. For use of bacterial probes, tipless or colloidal cantilevers are common [10].

1.6 Aim of study

The aim of this study was to investigate the adhesion abilities of the common salmonid pathogens *A. Salmonicida* and *Y. Ruckeri* to the skin and gut mucosa of Atlantic salmon. AFM operated in force spectroscopy mode was used to measure the molecular interactions occurring between the pathogens and extracted mucins, and between *A. Salmonicida* and the intact skin mucus layer of salmon fry. Moreover, extracted mucins were treated with neuraminidase to remove sialic acids from the mucins to investigate the role of these molecules in adhesion events. Producing a bacterial probe with a dense cover of bacteria had proved to be challenging for previous master students using bacterial probes in AFM measurements [63, 64]. For this reason, another sub-aim of this study was to establish a method to immobilize bacteria that would yield a dense cover. The main objective of the experiments executed in this these was to obtain a better understanding of the initial stage, namely the adhesion stage, of fish infections. The particular pathogens were selected due to their relevance in infections and high mortality in fish.

Materials and methods

2.1 Cultivation of bacteria

The bacteria studied in this thesis were *Aeromonas Salmonicida*, *Yersinia Ruckeri*, *Janthinobacterium Lividum* and *Arthrobacter* sp. *A. Salmonicida* was provided by Sara Linden and Janos Tamas Padra (Deptartment of Medical Chemistry and Cell Biology, University of Gothenburg) and *Y. Ruckeri* was provided by Alexander Fiedler (PhD student, Department of Biotechnology and Food Science, NTNU). *J. Lividum* and *Arthrobacter* sp. was isolated from the skin of adult Atlantic Salmon and identified through 16S RNA analysis by Mia Tiller Mjøs (Engineer, Department of Biotechnology and Food Science, NTNU).

The different bacterial strains were stored in glycerol stocks at -80°C. The particular glycerol stocks were prepared by adding bacteria grown in tryptic soy broth (TSB, VWR chemicals) medium overnight, with 15% glycerol (Sigma-Aldrich) and subsequently freezed. When used, each strain was plated on tryptic soy agar (TSA, Sigma-Aldrich) plates and incubated for 48 hours at 21°C. The bacteria were then transferred to TSB medium and left to grow for 24-48 hours at 21°C to achieve a dense culture. The lids of the culture tubes where attached loosely to maintain an aerobic environment inside the tube and allow optimal growth conditions.

2.2 Dialysis of Atlantic salmon mucins

Skin mucins (1 mg) and proximal intestinal mucins (1 mg) isolated from adult Atlantic salmon were provided by Sara Linden and coworkers. The mucins were stored in

guanidine hydrochloride (GuHCl, 4 M, Sigma-Aldrich) during shipment. Dialysis was used to change media to phosphate buffered saline (PBS, PH $\sim$ 7.4, Sigma-Aldrich).

The same procedure was executed for both types of mucins. A dialysis tube was placed in Milli-Q (MQ) water for 10 minutes. A clamp was put on the end of the tube and it was rinsed thoroughly with sterile MQ water. Mucin solution was added to the tube and closed with another clamp. The closed tube was first dialyzed against GuHCl (4 M) for 12 hours, to keep the sterilty of the mucins. Further dialysis was done against NaCl (2 M) for 2x12 hours, followed by NaCl (0.5 M) for 8 hours. Final dialysis was executed against the PBS buffer 2x4 hours in a cold room. All the buffer changes were done in a sterile hood. Both mucins were aliquoted into 50 µg and stored in the freezer.

2.3 Immobilization of bacteria to AFM probes

Two different methods for immobilization of bacteria to AFM probes were tested. This was done to investigate which of the methods that could provide the densest cover of bacteria, and thus be used to prepare probes for the AFM experiments. Differences and similarities between the two methods are shown in table 2.1.

Table 2.1: The different conditions used in the two procedures tested for immobilization of bacteria. Conditions include the type of chemical adherent, the incubation time after addition of this chemical adherent, if the process of centrifugation was utilized to harvest bacteria (+/-) and the incubation time after adding bacteria.

	Chemical adherent	Incubation time chemical adherent	Centrifugation	Incubation time bacteria
Method 1	PDA (4 mg/mL)	45 min	+	20 min
Method 2	PDA (4 mg/mL)	45 min	-	Overnight

2.3.1 Method 1: Immobilization of bacteria using 20 minutes incubation

PNP-TR-TL tipless cantilevers (NanoAndMore GmbH, appendix C.1) were covered with 100 µL PDA (4 mg/mL) dissolved in Tris buffer. This was left on for 45 minutes before it was removed and the tips were subsequently rinsed with MilliQ. The two types of bacteria, *J. Lividum* and *Arthrobacter* sp. were harvested through centrifugation. 1 mL of each of the liquid bacterial cultures was added to eppendorf tubes and centrifuged (2000 rpm, 22°C, 5 minutes). The supernatants were removed and the pellets were resuspended with 1 mL PBS. This step was repeated once. 100 µL of the bacterial solutions were added to each cantilever and left to adhere for 20 minutes. The probe was then washed with PBS to remove bacteria that was not attached.

2.3.2 Method 2: Immobilization of bacteria using overnight incubation

Dopamine hydrochloride (Sigma-Aldrich) was dissolved in Tris buffer to yield a concentration of 4 mg/mL. This solution of PDA was added onto AFM cantilevers and left to adhere for 45 minutes. The solution was removed and subsequently washed with MQ. Filter paper was gently used to remove the rest of the solution. 20 µL of the bacteria *J. Lividum* and *Arthrobacter sp.* was added onto each tip directly from the liquid suspensions. The bacteria were left to immobilize on the probe for 12 hours at 21°C. The probe was washed with PBS to remove unattached bacteria before use.

2.3.3 Live/dead assay of bacteria immobilized to AFM probes

To investigate which method gave the best cover of immobilized bacteria on the cantilever, live/dead stain and fluorescence microscopy was used. The presence and viability of bacteria was verified by using L7012 LIVE/DEAD® Bac-Light Bacterial Viability Kit (Invitrogen) to stain the bacteria and study it by microscopy using Zeiss Axio Observer

Z1. The kit includes two stains, SYTO 9 and propidium iodide. A mixture of the two stains ensure that live bacteria with intact cell membranes emit green fluorescent light from the fluorophore SYTO 9, whereas bacteria with damaged cell membranes emit red fluorescent light due to the fluorescent intercalating agent propodium iodide which binds to DNA.

Live/dead assay was performed on the AFM probes immobilized with bacteria by method 1 and 2. Equal volumes of component A and component B were mixed in an Eppendorf tube to get a final volume of 3 µL. To prevent the stain from interfering with the adhesion of bacteria to the probe, the mixture was added to the already prepared probes and not into the bacterial suspension as instructed by the manufacturers. 1 mL of salmon gnotobiotic medium (SGM, appendix A) was added to the mixture and the cantilevers were covered with 100 µL of this solution. The stain was left on for 20 min in a dark environment, to prevent photobleaching of the dye. It was then washed with SGM.

The probes were studied with Zeiss Axio Observer Z1. The objective 20x was used with the filters brightfield, Syl9 and PI. Syl9 was used to visualize the live bacteria stained with SYTO 9, PI was used to present the cells stained with propidium iodide and brightfield was used to get a clear image of the tip.

2.4 AFM force spectroscopy to study adhesion interactions between pathogenic bacteria and mucins

Adhesion properties of pathogenic bacteria to mucins were quantified using AFM force spectroscopy. The adhesion interactions of *A. Salmonicida* and *Y. Ruckeri* to mucins found in Atlantic salmon fish skin and proximal intestine were examined. The mucins were also treated with neuraminidase (neuraminidase from Arthrobacter ureafaciens, Sigma Aldrich) to see if the removal of sialic acids would affect the binding. Each bacteria was measured against both mucins, with and without neuraminidase treatment.

A simplified version of the experimental setup is shown in figure 2.1

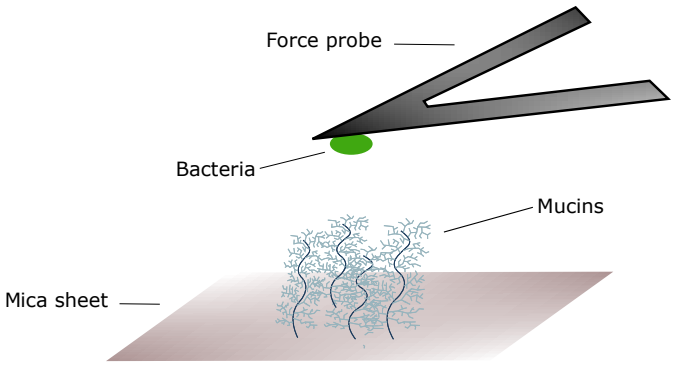

Figure 2.1: Illustration of the setup used for AFM force spectroscopy measurements between bacteria and mucins. Bacteria were immobilized on a tipless cantilever, and Atlantic salmon mucins were fixed to a mica sheet and covered with SGM. Some measurements were executed on mucins which were treated with neuraminidase after immobilization to the mica sheet.

2.4.1 Immobilization of bacteria to AFM probes

50 µL solution of polydopamine hydrochloride (4 mg/ml in Tris buffer) was used to cover the tipless AFM cantilever. The solution was left to polymerize for 45 minutes, and subsequently washed with MQ and dried with filter paper. 20 µL bacteria, either *A. Salmonicida* or *Y. Ruckeri*, was added to the probe and incubated for 12 hours at 21°C.

2.4.2 Coating of mica surfaces with mucins

The mucins, isolated from salmon skin and proximal intestine, were fixed to mica surfaces using the procedure described in the following. Freshly separated mica sheets were incubated with 250 µL of a solution with 6 µL N-[3-Trimethoxysilyl)propyl]ethyl-enediamine triacetic acid trisodium salt (silane-COOH, abcr Gmbh) in 494 µL acetic acid (1 mM, Sigma-Aldrich) for 20 minutes and washed with acetic acid. The mucins were dissolved in boric acid (50 mM, pH 5.8, Sigma-Aldrich) to a final concentration of

0.25 mg/mL with 0.5 mg/mL N-(3-Dimethylaminopropyl)-N'-ethylcarbodimide hydrochloride (EDC, Sigma-Aldrich). The mucins were applied to each mica sheet and left to adsorb for 1.5 hours. Excess solution was pipetted off and MQ was used to wash the sheets. The two mica sheets covered with mucins were glued onto small glass Petri dishes with JPK bio-compatible glue (Bruker Nano GmbH) or superglue. For the JPK glue the two components were mixed 1:1 and once applied to the surfaces, it was left to dry for 15 minutes. The Petri dishes were then filled with 3 mL SGM to prevent the mucins from drying out.

2.4.3 Neuraminidase treatment on mucins

Neuraminidase solution was diluted in the provided reaction buffer according to manufacturer's instructions. 2 units of neuraminidase in buffer was added to each mucin-coated surface and incubated at 37 °C for 30 min before rinsing the surface thoroughly with SGM.

2.4.4 Collection of curves

A Forcerobot©300 (JPK, Bruker Nano GmbH) was used for AFM measurements. Bacteria, *A. Salmonicida* or *Y. Ruckeri*, were immobilized to a tipless AFM cantilever, as described in section 2.4.1 and washed with SGM before use in AFM. The mucins, skin or proximal intestinal, with or without treatment with neuraminidase, were functionalized on a mica surface as described in section 2.4.2 and placed under the AFM after calibration of the tip.

Some AFM parameters were kept constant for all measurements, including no retraction delay, no extend relay, and a Z-length of 3. Detector sensitivity and spring constant are values that vary between probes and needed to be determined for each one used. The detector sensitivity was found by approaching the tip to a clean glass surface, and the spring constant of the cantilever was determined based on the thermal noise method. Intervals of values for sensitivity and spring constants for all the probes used are shown

in table 2.2. Approximately 1000 curves were obtained per measurement.

Table 2.2: Intervals for the sensitivity (nm/V) and spring constant (N/m) for the probes used in the experiments. Values were obtained by calibration of the cantilevers.

Parameter	Value
Sensitivity (nm/V)	32.33 - 88.62
Spring constant (N/m)	0.032 - 0.086

2.4.5 Analysis of curves

The force curves obtained from the AFM measurements were analyzed with JPK SPM data processing software. Curves containing molecular interactions with a straight baseline were processed, while curves without interaction or a high amount of noise were discarded. The percentages of curves containing interactions were calculated from the total amount of curves, excluding the ones discarded due to noise. The JPK analysis yielded a text file with measurements of the deadhesion work for each processed curve. The deadhesion work data were presented by histograms, displaying the distribution of deadhesion work. These histograms were made with SigmaPlot 14.0.

IDL was used to analyze the rupture force and loading rate for each interaction. Files obtained from JPK processing software were analyzed with the program difordisjpk-v31dr3 written by Bjørn Torger Stokke (Professor, Department of physics, NTNU) to obtain rupture forces. Force curves may have several rupture events (peaks) due to multiple interactions being ruptured. This program can be used to measure individual peaks. The rupture force (nN) is found from the height of the force peak relative to the baseline, and the loading rate (nN/s) is defined as an external force applied per unit of time, which can be calculated from the slope of the curve. After analysis with IDL, SigmaPlot 14.0 was used to create histograms presenting the frequency of rupture force strengths, as well as scatter plots with rupture forces plotted against loading rates of the interactions. The IDL program DiForDisMultiJPK3, also provided by Bjørn Torger

Stokke, was used to present selected force-distance curves.

2.4.6 Live/dead assay of bacteria immobilized to probes after use in AFM

A consequence of doing experiments with the AFM using bacteria immobilized on AFM cantilevers, is that the bacteria might die or fall off during the experiment. To ensure that the bacteria were still attached and alive after experiments, the tips were dyed with live/dead stain and pictures were taken with Zeiss Axio Observer Z1, the same way as described in section 2.3.3.

2.5 AFM force spectroscopy to study adhesion interactions between pathogenic bacteria and skin mucosa of Atlantic salmon

Adhesion properties of the pathogenic bacteria *A. Salmonicida* to fish skin mucosa were quantified using AFM force spectroscopy. Three different types of salmon fry that had been raised under different conditions were studied: Germ-free (GF), conventionally raised (CVR) and conventionalized (CVZ). GF were kept sterile throughout the yolk-sac stage, CVR were kept with their original bacterial content, while CVZ were treated as GF but had bacteria reintroduced one week post hatching. GF, CVR and CVZ Atlantic salmon fry were provided by Sol Gomes de la Torre Canny (Scientist, Department of Biotechnology and Food Science, NTNU), and the cultivation of Atlantic salmon fry is described in appendix B. The different conditions influence the fish's growth and development, including the mucus layer and its adhesion properties. Measuring the adhesion between *A. Salmonicida* and the three different types of fish were done to examine the adhesion of this bacteria to mucus and to investigate the potential variation in adhesion to the different types of fish. All the fish used in experiments were 8 weeks

old. A simplified version of the experimental setup is shown in figure 2.2

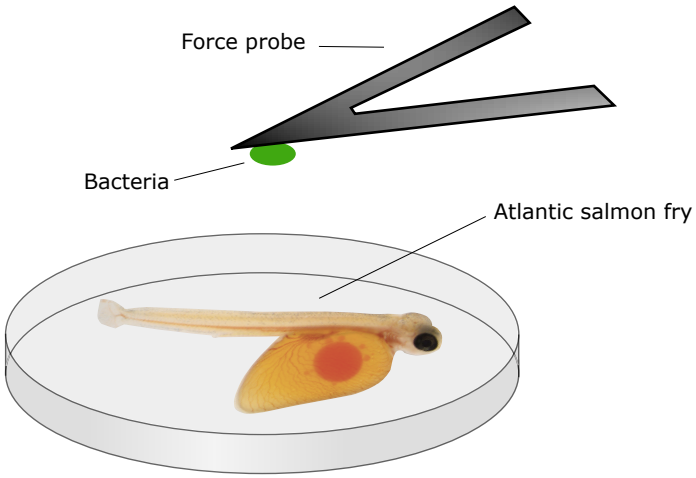

Figure 2.2: Illustration of the setup used for AFM force spectroscopy measurements between bacteria and Atlantic salmon fry. Bacteria were immobilized on a tipless cantilever, and Atlantic salmon fry was immobilized in a Petri dish with agarose gel, and covered with SGM.

2.5.1 Preparation of fish

The fish was euthanized in Ethyl 3-aminobenzoate methanesulfonate (Tricaine, Sigma-Aldrich). A stereo microscope Olympus SZX10 was used to observe that the skin was intact and that the heartbeat stopped before proceeding. An image of a 9 week old fish fry obtained with this microscope is shown in figure 2.3, which shows the heart, yolk sac, fins, skin surface and tails. After observation in the microscope, the fish was rinsed with SGM and put into a small glass Petri dish. 1 mL of low-melt agarose gel (mp $\leq$65 °C at a 1.5% gel, Sigma-Aldrich) was melted in a water bath. This was used to immobilize the fish by pipetting it onto the dish and around the fish, leaving the skin surface exposed. To solidify the gel, the sample was put in a refrigerator for 5 minutes. 3 mL of SGM was added to the dish and the sample was ready for AFM measurements.

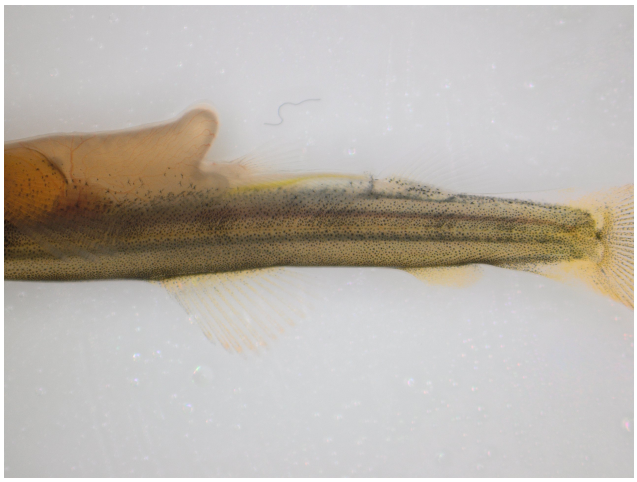

Figure 2.3: The surface of a 9 weeks old Atlantic salmon fry. The picture is taken with the microscope Olympus SZX10, and shows the skin, heart, yolk sac, fins and tail. Photo by Karen Dunker.

2.5.2 Collection of curves

A Forcerobot©300 (JPK, Bruker Nano GmbH) was used for AFM measurements. Three fish of each type, GF, CVR and CVZ, were studied with probes covered with *A. Salmonicida*. Each probe was immobilized with bacteria and washed with SGM as described in section 2.4.1, and subsequently mounted in the AFM. The fish was prepared as described in section 2.5.1 and placed in the AFM.

Force-distance curves were measured at three different areas of each fish. The main body covered in skin was measured, avoiding the fins, yolk sac and tail. To visualize the position of the cantilever on the fish skin, the camera function in JPK software was used, and a flashlight helped illuminate the fish, shown in figure 2.4. This was done to find suitable areas to obtain samples. The total of curves obtained varied from 100-500 depending on the quality of the curves obtained. Some AFM parameters were kept constant for all measurements, including no retraction delay, no extend relay, and a Z-length of 10. The detector sensitivity and spring constant varied for each probe. The detector sensitivity was found by approaching the tip to a clean glass surface, and the spring constant of the cantilever was determined based on the thermal noise method. Intervals of these values are shown in table 2.3

Table 2.3: Intervals for the sensitivity (nm/V) and spring constant (N/m) for the probes used in the experiments with fish. Values were obtained by calibration of the cantilevers.

Parameter	Value
Sensitivity (nm/V)	49.82 - 69.53
Spring constant (N/m)	0.037 - 0.057

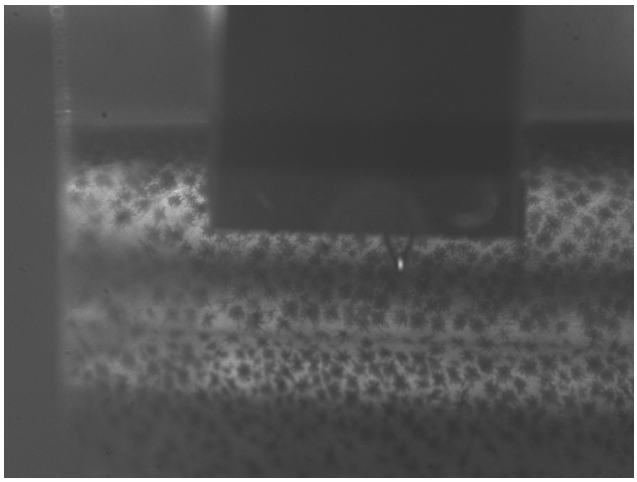

Figure 2.4: Salmon fry mounted in the AFM during collection of curves. The large triangle is the cantilever in use, and the bright spot is the position of the laser. The area underneath with a grey surface and dark spots is the skin of the salmon fry. Photo by Tove Enmo Bugge.

2.5.3 Analysis of curves

The IDL program DiForDisMultiJPK3 was used to present selected force-distance curves. The deadhesion work and rupture force could not be calculated as there were no recorded interactions.

Results

The aim of this study was to investigate the adhesive properties of the pathogenic bacteria *A. Salmonicida* and *Y. Ruckeri* to Atlantic salmon extracted skin and proximal intestinal mucins and the skin mucus of germ-free (GF), conventionally raised (CVR) and conventionalized (CVZ) Atlantic salmon fry. Also, the extracted Atlantic salmon mucins were treated with neuraminidase to remove sialic acids, with the objective to investigate the effect this removal had on bacterial adhesion to the mucins. The adhesion between the bacteria and the mucins or skin mucus was quantified by AFM force spectroscopy. The first aim of the study was to identify appropriate method for immobilizing and creating a layer of bacteria on the AFM probes. This was achieved by testing two different methods and inspecting the density and viability of the bacteria with fluorescent microscopy.

3.1 Immobilization of bacteria to AFM probes

Two methods were tested for immobilization of the gram-negative *J. Lividium* and the gram-positive *Arthrobacter* sp. to PNP-TL-TR tipless AFM cantilevers. Live/dead stain and fluorescence microscopy were used to observe the density and cover of bacteria on the AFM probes, as well as checking the viability of the immobilized microbes. This was performed to investigate which method gave the best cover of immobilized bacteria to the surface of the AFM cantilevers. Images from both methods with the two bacteria were obtained, as well as a negative control where a PDA treated probe without bacteria was stained and imaged. The negative control is shown in appendix C.2, and shows that without addition of bacteria, no fluorescent light was emitted.

3.1.1 Method 1

Images of the live/dead assay performed on *Arthrobacter* sp. and *J. Lividium*, immobilized on probes with method 1, is shown in figure 3.1. For both types of bacteria there are very few or no bacteria attached to the tip. The few bacteria observed are positioned near the chip and not the tip of the cantilever as intended. The majority of the observed cells emitted green fluorescence, while very few emitted red light, thus indicating that most of the bacteria were alive and remained viable after immobilization.

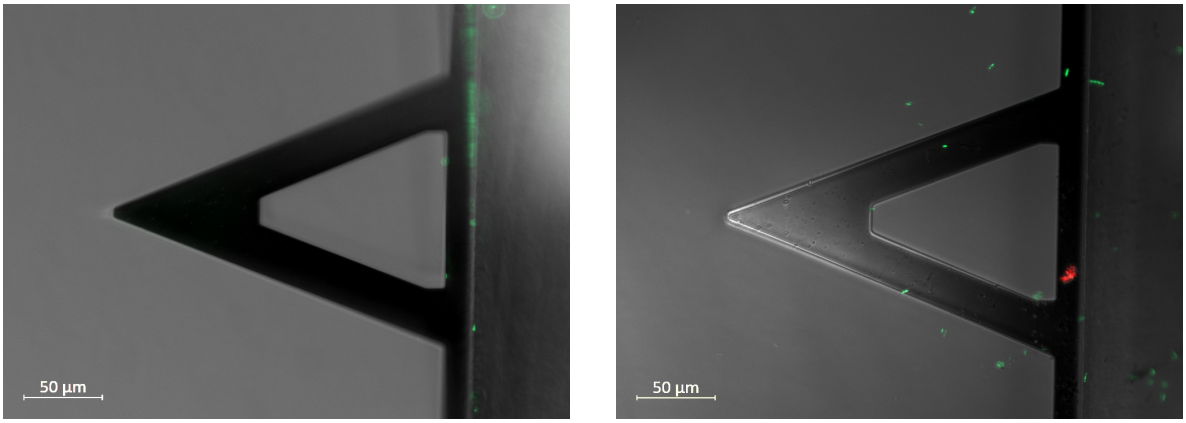

Arthrobacter sp. *J. Lividium*

Figure 3.1: Live/dead assay of *Arthrobacter* sp. and *J. Lividium* immobilized on PDA-treated tipless AFM cantilevers with 20 minute incubation. Green fluorescence is emitted from live bacteria, while red fluorescence is emitted from dead bacteria. Images are obtained with Zeizz Axio Observer Z.1 microscope with a 20X objective.

3.1.2 Method 2

The second method provided a high amount of immobilized bacteria on the cantilever surface. The cover of gram-positive *Arthrobacter* sp. were denser than with the previous method, and the bacteria were distributed on the tip, shown in figure 3.2a. The gram-negative *J. Lividium* provided a slightly thinner cover than *Arthrobacter* sp., shown in figure 3.2b. Most of the bacteria emitted green light, indicating that the long incubation time did not affect the viability of the bacteria.

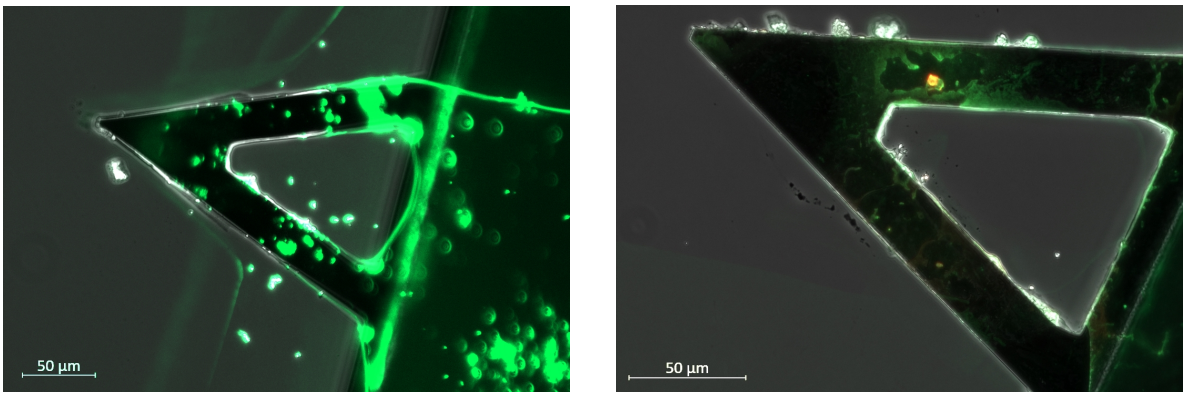

Arthrobacter sp. *J. Lividium*

Figure 3.2: Live/dead assay of *Arthrobacter* sp. and *J. Lividium* immobilized on PDA-treated tipless AFM cantilevers with overnight incubation. Green fluorescence is emitted from live bacteria, while red fluorescence is emitted from dead bacteria. Images are obtained with Zeizz Axio Observer Z.1 microscope with a 20X objective.

Both methods provided viable bacteria deposited on the AFM cantilever, but the density of immobilized bacteria varied strongly. The first method gave almost no immobilized bacteria, while the second method yielded a denser cover of bacteria. Thus, the second method was used to prepare probes for the AFM force spectroscopy experiments.

3.1.3 Probes after use in AFM

Some tips were stained with live/dead after use in AFM, and observed in the microscope. This was performed to ensure that bacteria were still attached and alive after experiments. Moreover, comparing images of the probe used for AFM experiments could be used to support results found by the force spectroscopy experiments. Figure 3.3 shows images from seven probes used in AFM experiments. Probes that are not presented in this figure were not imaged after use in the AFM. Even though the method used for experiments (method 2) gave good results during method development, the amount and position of bacteria attached varied between different probes used in experiments. The cover of bacteria on the probes are presented in this section, and the results from the AFM measurements executed with these probes are presented later in this thesis.

Three probes are from the AFM measurements of interactions between *Y. Ruckeri* - neuraminidase treated (NeuT) mucins (figure 3.3i-iii). The probe used in parallel B (figure 3.3ii) was distinct from the other two probes as it had a large collection of bacteria positioned at the tip of the cantilever. The probe used in parallel A (figure 3.3i) also had a a cluster of bacteria, but this was positioned closer to the chip than the tip. The probe from parallel C (figure 3.3iii) had a more evenly distributed cover, however relatively few bacteria were attached. Results for deadhesion work obtained from these measurements are shown in figure 3.13.

Two probes used in experiments with *A. Salmonicida* - NeuT mucins (figure 3.3 iv-v) were imaged after use. These two had similar covers of bacteria on the tip, although the probe from parallel B (figure 3.3iv) was more dense and had a higher amount positioned at the tip, than the one from parallel C (3.3v). Results for deadhesion work obtained from measurements with these probes are shown in figure 3.11.

The probe utilized in parallel C for experiments with *Y. Ruckeri* - mucins (figure 3.3vi), had some bacteria on the cantilever and a spot at the tip with bacteria clustered together. Results for deadhesion work obtained from experiments with *Y. Ruckeri* - mucins are shown in figure 3.7.

A few, evenly distributed bacteria were spotted on the cantilever used for parallel C of experiments between *A. Salmonicida* - mucins (figure 3.3vii). Results for deadhesion work obtained from experiments with *A. Salmonicida* - mucins are shown in figure 3.5.

The bacteria emitted both green and red color, indicating that some were alive and some were dead. In the areas where bacteria clustered, yellow light was observed. This is a result of live and dead bacteria being present in that area, where the combination of emitted green and red light gave yellow color. Most of the areas emitting red also have a slight glimpse of yellow, showing that some bacteria might still be alive in that area as well. This means that there were live bacteria in the majority of areas where bacteria was observed, even after long-lasting use in the AFM.

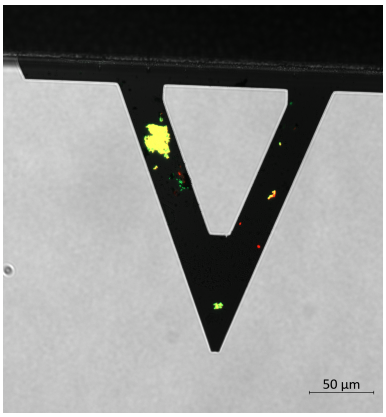

i. *Y. Ruckeri* - NeuT mucins (Parallel A)

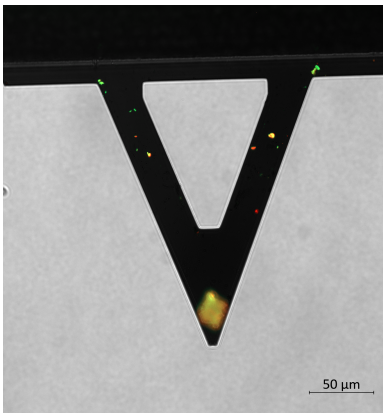

ii. *Y. Ruckeri* - NeuT mucins (Parallel B)

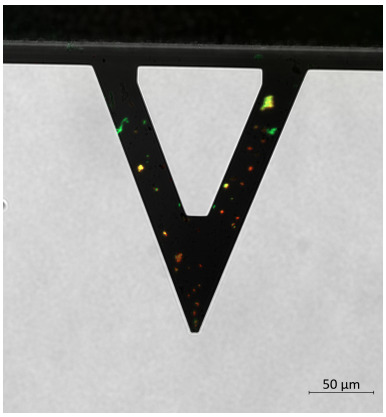

iii. *Y. Ruckeri* - NeuT mucins (Parallel C)

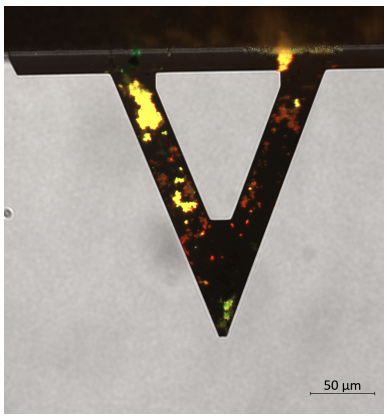

iv. *A. Salmonicida* - NeuT mucins (Parallel B)

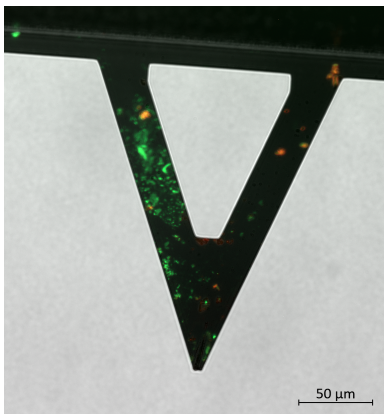

v. *A. Salmonicida* - NeuT mucins (Parallel C)

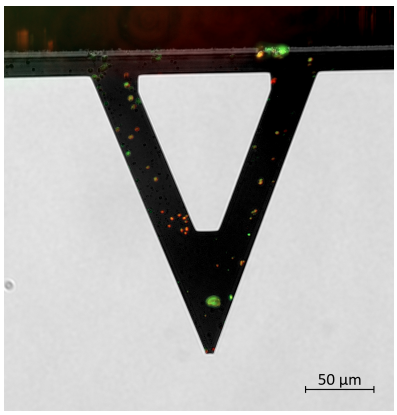

vi. *Y. Ruckeri* - mucins (Parallel C)

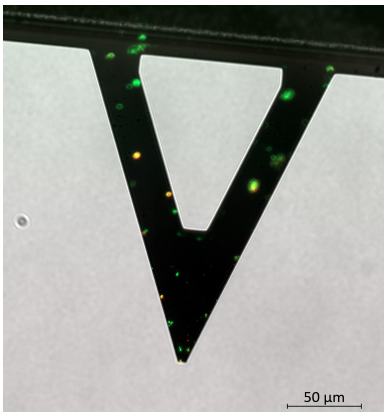

vii. *A. Salmonicida* - mucins (Parallel C)

Figure 3.3: Live/dead assay of AFM cantilevers after they have been used in AFM experiments. The type of attached bacteria and the specific parallel the probe has been used in is described in the subcaption. i-iii are from experiments with *Y. Ruckeri* - NeuT mucins, iv-v are from experiments with *A. Salmonicida* - NeuT mucins, vi is from an experiment with *Y. Ruckeri* - mucins, while vii is from an experiment with *A. Salmonicida* - mucins. Green fluorescence is emitted from live bacteria, while red fluorescence is emitted from dead bacteria. Images are obtained with Zeizz Axio Observer Z.1 microscope with a 20X objective.

3.2 Adhesion of pathogenic bacteria to Atlantic salmon mucins

Adhesion interactions of the pathogenic bacteria *A. Salmonicida* and *Y. Ruckeri* to mucins were measured with AFM force spectroscopy. Two types of mucins were investigated, skin and proximal intestinal (gut), both isolated from Atlantic salmon. Interactions for each bacteria with both types of mucins were measured. The same probe covered with one type of bacteria was used in measurements with skin mucins and gut mucins to compare the adhesion interactions for the two types. Three replicates of measurement of each adhesion pair were executed on different days. For each replicate a new, freshly prepared probe was used. Approximately 1000 force-distance curves were obtained per mucin. For each adhesion pair the percentage of curves containing interactions, force-distance curves, and the distribution of deadhesion work were presented. For some interactions, the rupture force was determined.

3.2.1 *A. Salmonicida* - mucins

AFM force spectroscopy of *A. Salmonicida* covered probes to mucin coated mica surfaces gave a relatively high amount of curves containing interactions, for both types of mucins. The percentages of force-distance curves containing interactions from each parallel are shown in table 3.1. For both skin and gut mucins the percentages varied, ranging from 40-90 %. The probe used in parallel C was imaged after use, shown in figure 3.3vii.

Table 3.1: Percentages of force-distance curves containing interactions, from measurements between *A. Salmonicida* and Atlantic salmon skin or gut mucins. A, B and C represent three different replicates of measurement, where each parallel used a new, freshly prepared probe.

Parallel	Curves containing interactions (%)	
	Skin	Gut
A	93.2	42.5
B	86.0	90.4
C	47.3	70.1

A selection of force-distance retract curves obtained from measurements between *A. Salmonicida* and skin or gut mucins are shown in figure 3.4. Curves from the three replicates are represented, where i-iii are from parallel A, iv-vi are from B and vii-ix are from C. For both types of mucins, the majority of interactions have small single peaks, although some multiple force jumps were observed.

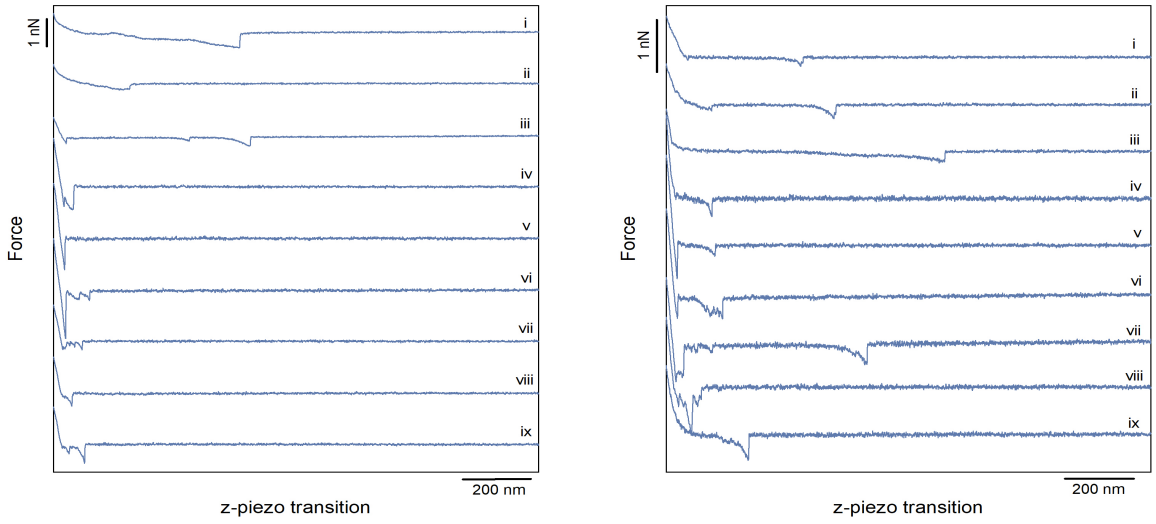

Figure 3.4: A selection of force-distance retract curves from interactions between *A. Salmonicida* and Atlantic salmon skin and gut mucins. Curves i-iii are from parallel A, iv-vi are from B and vii-ix are from C.

The amount of work required to break the interactions between *A. Salmonicida* and Atlantic salmon skin or gut mucins were found to be quite similar for both types of

mucins. Figure 3.5 shows histograms for each replicate of measurement, with deadhesion work plotted against the frequency of observations. Parallel A exhibits slightly higher deadhesion work for interactions with mucins from skin than gut, B shows very similar values, while C shows a somewhat greater amount of work executed on interactions with gut mucins than skin mucins. This illustrates that the amount of deadhesion work performed varied between replicates. Nevertheless, most of the deadheison work were in the same range, with the majority from 0-60 nN nm and the maximum value at around 140 nN nm. All parallels had a high frequency of deadhesion work with values from 0-10 nN nm.

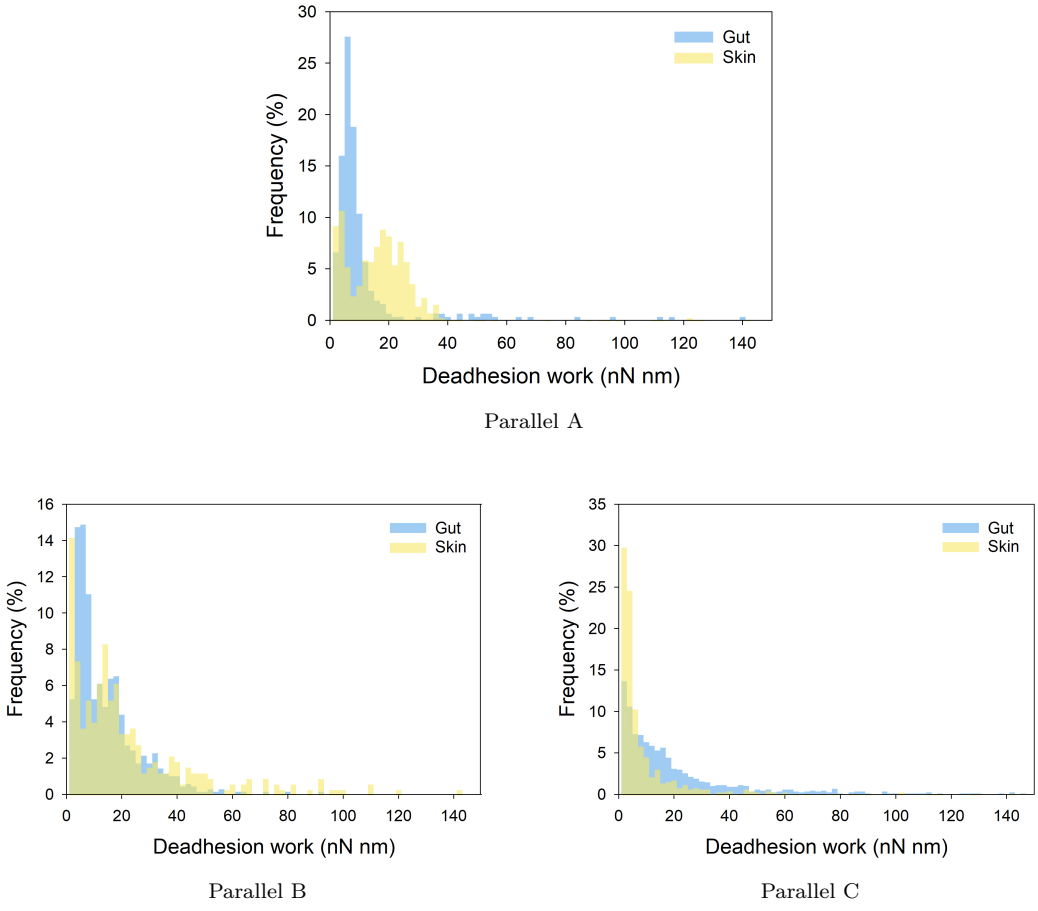

Figure 3.5: Deadhesion work for interactions between *A. Salmonicida* and Atlantic salmon skin (yellow) or gut (blue) mucins. The histograms display the distribution of deadhesion work (nN nm) for the interactions measured with AFM force spectroscopy. The different figures, A, B and C, represent three different replicates of measurement, where each parallel used a new, freshly prepared probe.

3.2.2 *Y. Ruckeri* - mucins

AFM force spectroscopy of *Y. Ruckeri* covered probes to mucin coated mica surfaces gave a very high amount of curves containing interactions, for both types of mucins. The percentages of force-distance curves containing interactions from each replicate of measurement are shown in table 3.2. All the parallels had over 87% curves containing interactions. The probe used in parallel C was imaged after use, shown in figure 3.3vi.

Table 3.2: Percentages of force-distance curves containing interactions, from measurements between *Y. Ruckeri* and Atlantic salmon skin and gut mucins. A, B and C represent three different replicates of measurement, where each parallel used a new, freshly prepared probe.

Parallel	Curves containing interactions (%)	
	Skin	Gut
A	99.9	99.2
B	91.9	97.1
C	87.7	95.9

Galleries of selected force-distance retract curves obtained from measurements between *Y. Ruckeri* and skin or gut mucins are shown in 3.6. Curves from the three replicates are presented, where i-iii are from parallel A, iv-vi are from B and vii-ix are from C. For skin several multiple interactions were observed, although replicate C had some single peaks. Gut had a higher amount of single peaks than skin, although interactions from experiment C were different as it had several multiple and large rupture events.

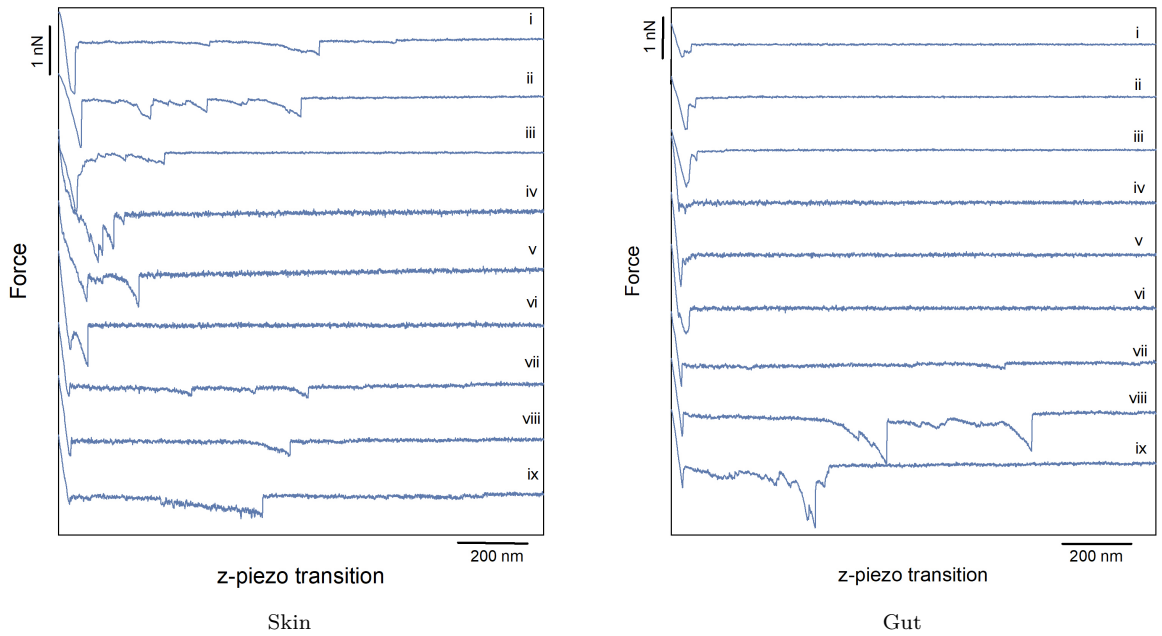

Figure 3.6: A selection of force-distance retract curves from interactions between *Y. Ruckeri* and Atlantic salmon skin and gut mucins. Curves i-iii are from parallel A, iv-vi are from B and vii-ix are from C.

The work required to retract the *Y. Ruckeri* covered probe from the mucin surface were found to be very different for the two types of mucins. The distribution of deadhesion work for each replicate of measurement is shown in figure 3.7. Experiment A and B gave similar results, the deadhesion work was found to be greater for interactions between the bacteria and skin mucins than that of the bacteria and gut mucins. Interactions with gut mucins gave a strong peak at 0-50 nN nm, while the interactions with skin were evenly distributed up to higher values of deadhesion work, with ∼150 nN nm for parallel A and ∼400 nN nm for parallel B. C differed from the other replicates, as the distributions of deadhesion work were more alike for the two types of mucins, and values for gut were placed towards slightly larger deadhesion work than skin. Even so, the general trend observed is that skin mucins, compared to gut mucins, require a higher amount of work to break the adhesive bonds to *Y. Ruckeri*.

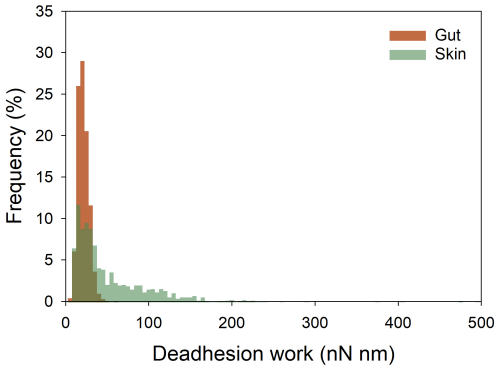

Parallel A

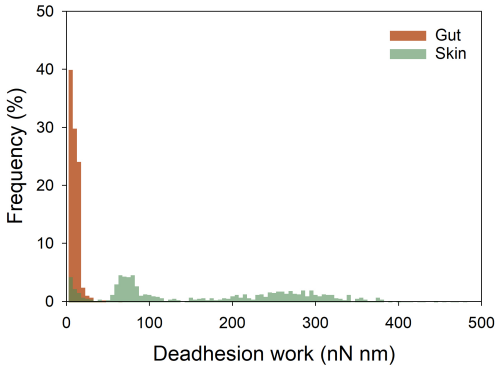

Parallel B

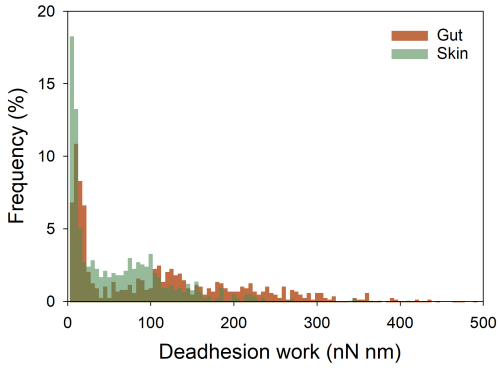

Parallel C

Figure 3.7: Deadhesion work for interactions between *Y. Ruckeri* and Atlantic salmon skin (green) and gut (red) mucins. The histograms display the distribution of deadhesion work (nN nm) for the interactions measured with AFM force spectroscopy. The different figures, A, B and C, represent three different replicates of measurement, where each parallel used a new, freshly prepared probe.

3.2.3 Rupture forces for *A. Salmonicida* - mucins and *Y. Ruckeri* - mucins

Force-distance curves obtained from one parallel of AFM experiments with *A. Salmonicida* or *Y. Ruckeri* to the Atlantic salmon mucins were processed with IDL to get the rupture forces and loading rates of individual peaks. These specific parallels were chosen due to their high amount of curves with single peaks, and not multiple interactions, since the analysis required well separated single rupture events. Scatter plots of rupture force plotted against loading rate of the different interactions are shown in figure 3.8.

Histograms showing the distribution of the experimentally determined rupture forces are shown in figure 3.9.

Interactions between the two bacteria and the two types of mucins had quite similar rupture forces, with the exception of *A. Salmonicida* to skin mucins, which were a bit weaker than the rest. The majority of interactions were in the range of 0.8 to 4.0 nN, with some outliers up to ∼8.0 nN. The recurrent peak at around 2.0 nN reveal that this was the most common rupture force value. Most of the loading rates ranged from 10-100 nN/s. Higher loading rates were connected to higher rupture force values.

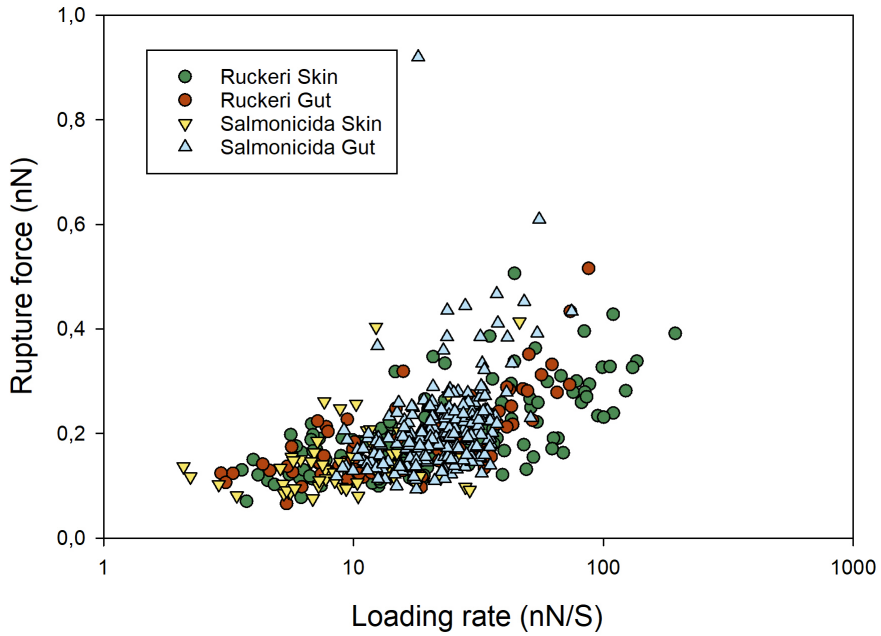

Figure 3.8: Rupture forces (nN) plotted against the force loading rate (nN/s) for interactions between *A. Salmonicida* or *Y. Ruckeri* and Atlantic salmon skin or gut mucins. Interactions were recorded with AFM force spectroscopy. The different shapes represent the type of bacteria, and the different colors represent the bacteria-mucin combination.

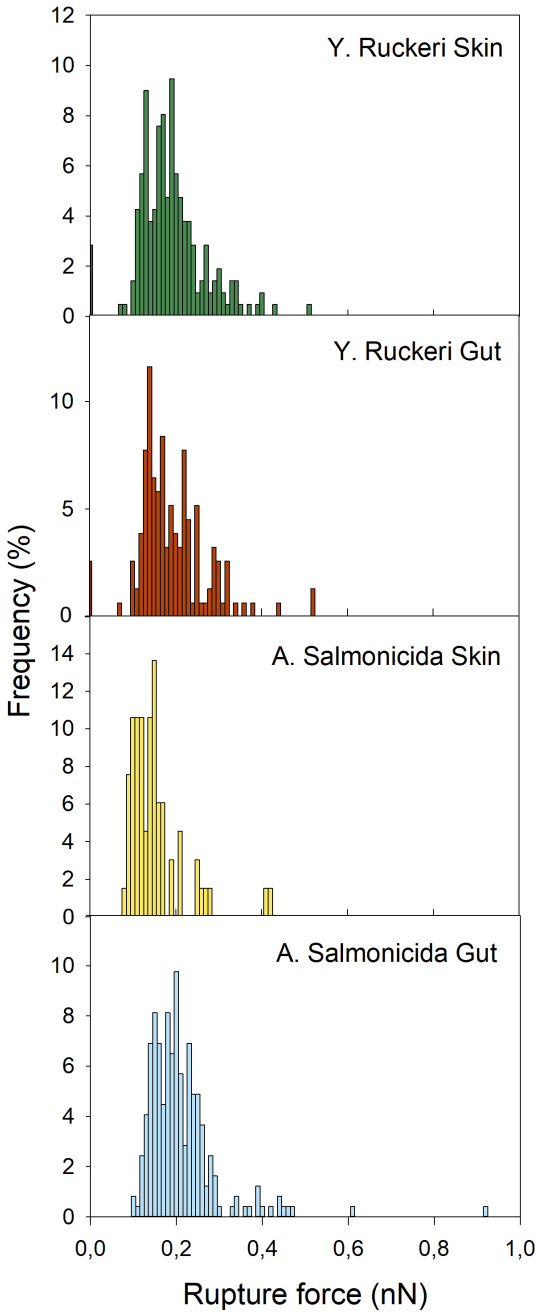

Figure 3.9: The distribution of inter-molecular rupture forces between *A. Salmonicida* or *Y. Ruckeri* and Atlantic salmon skin or gut mucins. Interactions were recorded with AFM force spectroscopy.

3.3 Adhesion of pathogenic bacteria to Atlantic salmon NeuT mucins

Adhesion of the pathogenic bacteria *A. Salmonicida* and *Y. Ruckeri* to Atlantic salmon mucins treated with neuraminidase were measured with AFM force spectroscopy. Two types of mucins were investigated, skin and proximal intestinal (gut), both isolated from Atlantic salmon. Both mucins were treated with neuraminidase to remove sialic acids shortly before experiments with the AFM. The same probe covered with one type of bacteria was used in measurements with both types of mucins to compare the adhesion interactions for the two types. Three replicates of measurements with each adhesion pair were executed on different days. Approximately 1000 force-distance curves were obtained per mucin. For each adhesion pair the percentage of curves containing interactions, force-distance curves, and the distribution of deadhesion work were presented. For some interactions, the rupture force was determined.

3.3.1 *A. Salmonicida* - NeuT mucins

AFM force spectroscopy of *A. Salmonicida* to NeuT mucins gave a high amount of curves containing interactions. The majority of parallels had over 70% curves containing interactions, shown in table 3.3. The probes used in parallel B and C were imaged after use, shown in figure 3.3iv-v.

Table 3.3: Percentages of force-distance curves containing interactions, from measurements between *A. Salmonicida* and Atlantic salmon skin and gut mucins treated with neuraminidase. A, B and C represent three different replicates of measurement, where each parallel used a new, freshly prepared probe.

Parallel	Curves containing interactions (%)	
	Skin	Gut
A	85.5	57.0
B	99.9	99.9
C	71.7	98.9

A selection of force-distance retract curves obtained from measurements between *A. Salmonicida* and NeuT skin or gut mucins are shown in figure 3.10. Curves from the three replicates are represented, where i-iii are from parallel A, iv-vi are from B and vii-ix are from C. Curves obtained from A and C were quite similar for both mucins, both exhibiting small, and mostly individual rupture events. Interactions from parallel B stands out as they have stronger rupture forces and multiple rupture events.

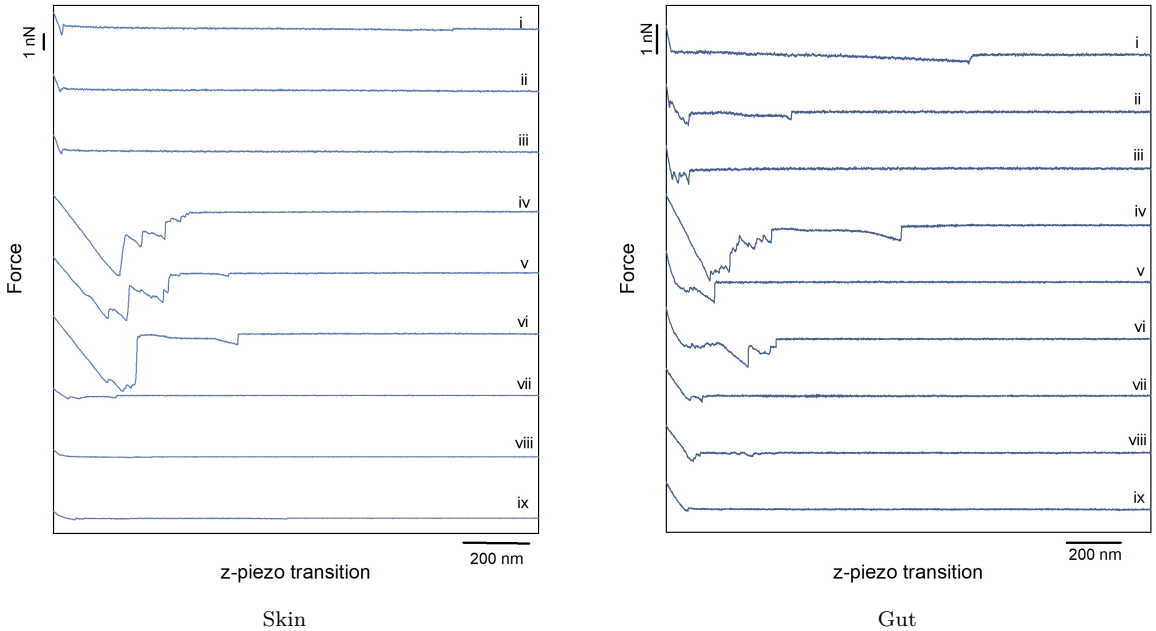

Figure 3.10: A selection of force-distance retract curves from interactions between *A. Salmonicida* and NeuT Atlantic salmon skin and gut mucins. Curves i-iii are from parallel A, iv-vi are from B and vii-ix are from C.

The work required to break the adhesion interactions between *A. Salmonicida* and the NeuT mucins, were quite different for the three replicates of the experiment. Histograms displaying the distribution of deadhesion work for the different parallels are shown in figure 3.11. Despite high variations between replicates, a recurring result is that the distribution of deadhesion work for interactions between *A. Salmonicida* and gut mucins are placed towards higher values than for the interactions between the bacteria and skin mucins. The amount of deadhesion work varies strongly between parallels, A has values up to approximately 600 nN nm, B up to around 1800 nN nm, and C has values at maximum 60 nN nm.

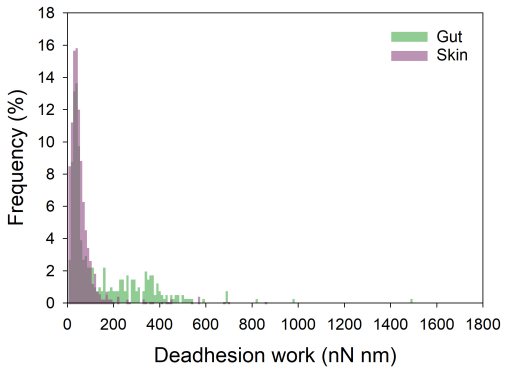

Parallel A

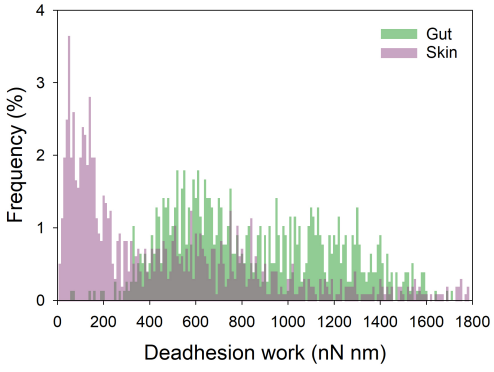

Parallel B

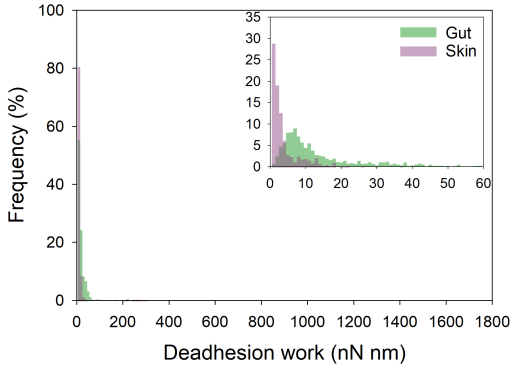

Parallel C

Figure 3.11: Deadhesion work for interactions between *A. Salmonicida* and NeuT Atlantic salmon skin (purple) or gut (green) mucins. The histograms display the distribution of deadhesion work (nN nm) for the interactions measured with AFM force spectroscopy. The different figures, A, B and C, represent three different replicates of measurement, where each parallel used a new, freshly prepared probe.

3.3.2 *Y. Ruckeri* - NeuT mucins

AFM force spectroscopy of *Y. Ruckeri* and NeuT mucins gave a high amount of curves containing interactions, for both types of mucins. The percentages of force-distance curves containing interactions from each parallel of measurementare shown in table 3.4. Parallel A and B had over 90% curves with interactions, and C had around 70%. The probes from all parallels were imaged after use, shown in figure 3.3i-iii.

Table 3.4: Percentages of force-distance curves containing interactions, from measurements between *Y. Ruckeri* and Atlantic salmon skin and gut mucins treated with neuraminidase. A, B and C represent three different replicates of measurement, where each parallel used a new, freshly prepared probe.

Parallel	Curves containing interactions (%)	
	Skin	Gut
A	96.8	94.7
B	93.9	90.5
C	71.1	68.0

Galleries of selected force-distance retract curves obtained from measurements between *Y. Ruckeri* and NeuT skin or gut mucins are shown in figure 3.12. Curves from the three replicates are represented, where i-iii are from parallel A, iv-vi are from B and vii-ix are from C. The curves are similar for both mucins, with small variations between parallels, although A exhibits smaller rupture events than the rest. The curves from replicate B appears to have more noise.

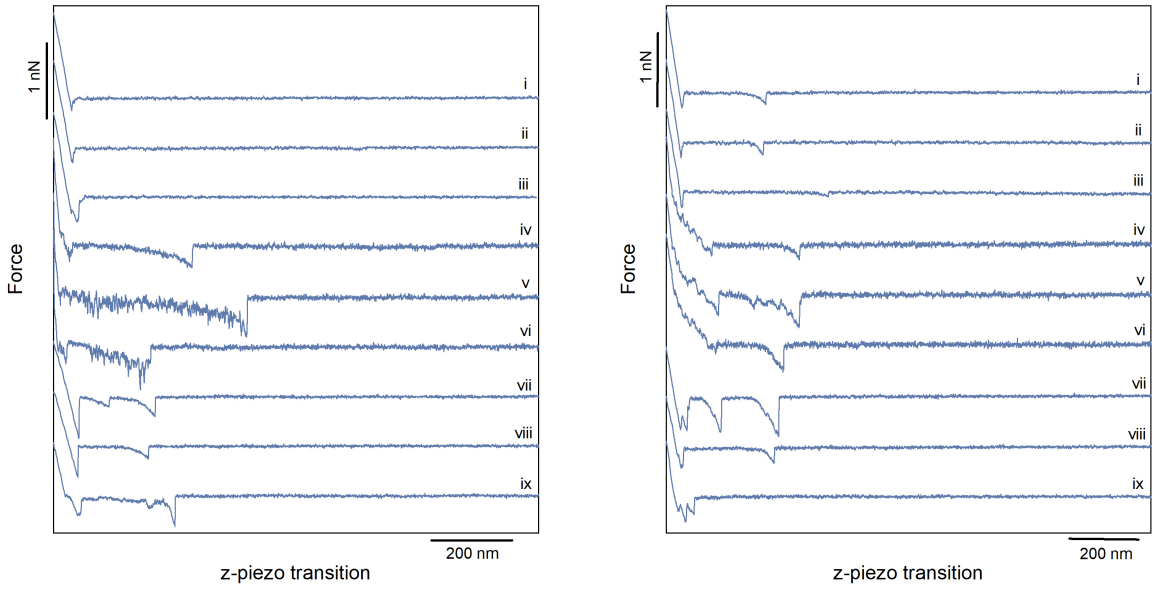

Figure 3.12: A selection of force-distance retract curves from interactions between *Y. Ruckeri* and NeuT Atlantic salmon skin and gut mucins. Curves i-iii are from parallel A, iv-vi are from B and vii-ix are from C.

The deadhesion work for interactions between *Y. Ruckeri* and mucins treated with neuraminidase varied between replicates. Figure 3.13 shows histograms for each parallel, with deadhesion work plotted against the frequency of observations. Parallel A shows no difference in deadhesion work between the two types of mucins. For both B and C the deadhesion work was found to be greater for interactions between the bacteria and skin than that of bacteria to gut. Common to all replicates was that interactions with gut required very low amounts of work to break the interaction, with a recurring peak at 0-5 nN nm. The values for skin varied more for the different parallels, A with a maximum of 5 nN nm, B with values up to 500 nN nm and C up ranging up to 150 nN nm.

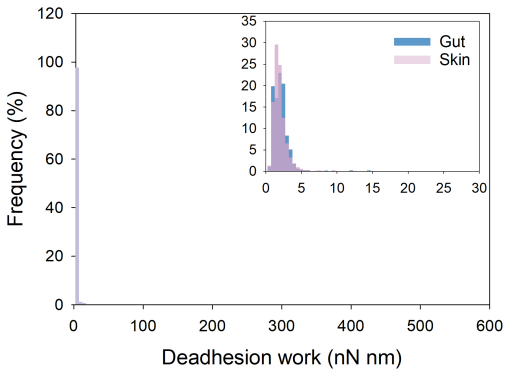

Parallel A

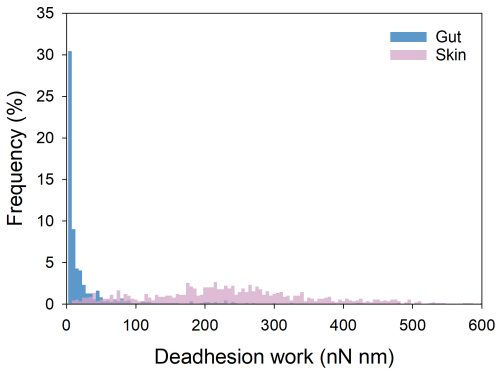

Parallel B

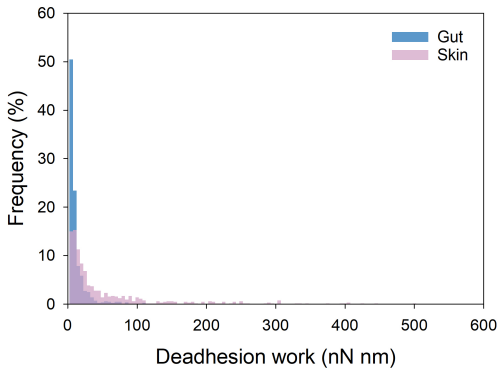

Parallel C

Figure 3.13: Deadhesion work for interactions between *Y. Ruckeri* and NeuT Atlantic salmon skin (pink) or gut (blue). The histograms display the distribution of deadhesion work (nN nm) for the interactions measured with AFM force spectroscopy. The different figures, A, B and C, represent three different replicates of measurement. where each parallel used a new, freshly prepared probe.

3.3.3 Rupture forces for *A. Salmonicida* - NeuT mucins and *Y. Ruckeri* - NeuT mucins

Force-distance curves obtained from one replicate of force spectroscopy measurement of *A. Salmonicida* or *Y. Ruckeri* to the NeuT Atlantic salmon mucins were processed with IDL to get the rupture forces and loading rates of individual peaks. These specific parallels were chosen due to their high amount of curves with single peaks, since the analysis required well separated single rupture events. Scatter plots of rupture force plotted against loading rate of the different interactions are shown in figure 3.14. Histograms showing the distribution of rupture forces are shown in figure 3.15.

Interactions between *A. Salmonicida* and mucins had a bit higher rupture forces than interactions between *Y. Ruckeri* and mucins. The majority of interactions were in the range of 0.1 to 0.4 nN, although interactions with *A. Salmonicida* had a peak at 0.2-03 nN and interactions with *Y. Ruckeri* had a peak at 0.1-0.2 nN. Most of the loading rates were in the range from 10-100 nN/s.

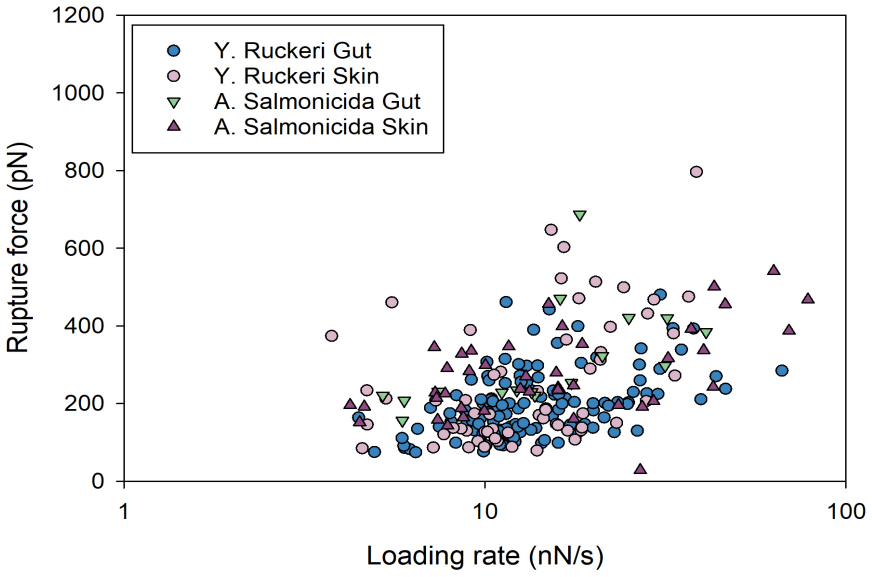

Figure 3.14: Rupture forces (nN) plotted against the force loading rate (nN/s) for interactions between *A. Salmonicida* or *Y. Ruckeri* and NeuT Atlantic salmon skin or gut mucins. Interactions were recorded with AFM force spectroscopy. The different shapes represent the type of bacteria, and the different colors represent the bacteria-mucin combination.

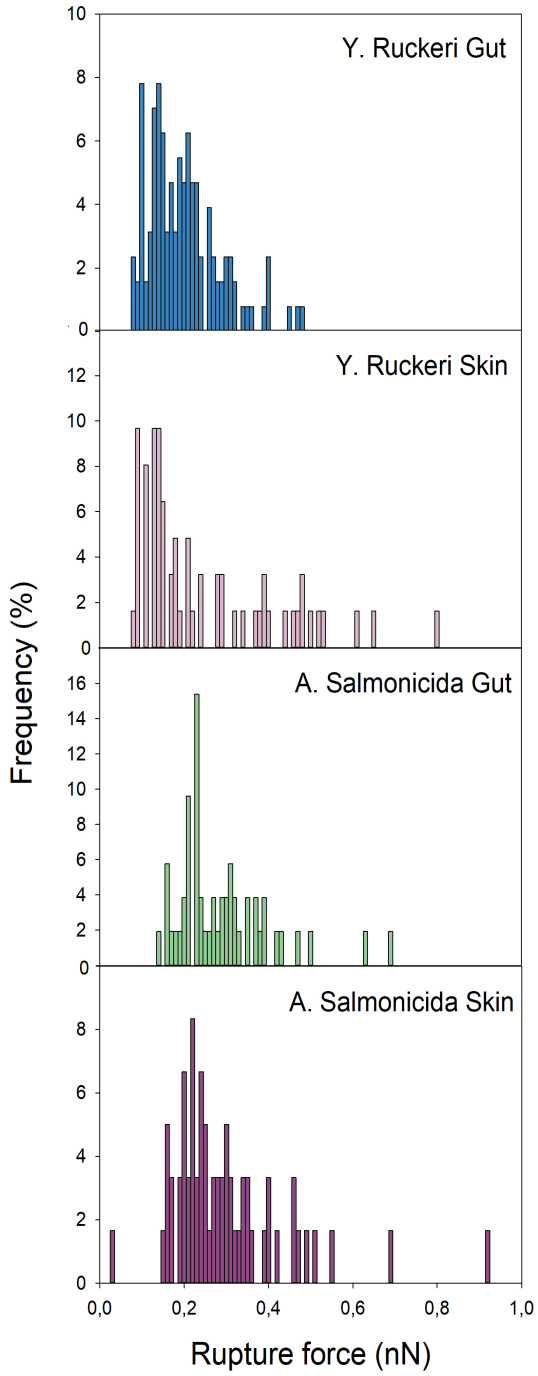

Figure 3.15: The distribution of inter-molecular rupture forces between *A. Salmonicida* or *Y. Ruckeri* and NeuT Atlantic salmon skin or gut mucins. Interactions were recorded with AFM force spectroscopy.

3.4 Comparison of pathogenic adhesion to Atlantic salmon mucins

Four combinations of adhesion pairs were measured with bacteria and the two types of mucins: *A. Salmonicida* - mucins, *A. Salmonicida* - NeuT mucins, *Y. Ruckeri* - mucins and *Y. Ruckeri* - NeuT mucins. Each of the combinations had three replicates of experiments, executed with different probes, and the results for deadhesion work have been combined to display the total and compare the different interactions. The distribution of deadhesion work for the four types of combinations to gut mucins are shown in figure 3.16, and to skin mucins are shown in 3.17. The frequency of the deadhesion work was modified for replicates to better portray the full extent of the interactions and avoid some values from becoming more predominant than the rest. Descriptions of the alterations are shown in Appendix D.

3.4.1 Pathogens - gut mucins

The distribution of the deadhesion work for *Y. Ruckeri*-gut mucin and *A. Salmonicida*-NeuT gut mucin interactions, are placed towards larger deadhesion work compared to *A. salmonicida*-gut mucin and *Y. Ruckeri*-NeuT gut mucin interactions, shown in 3.16. Deadhesion work for interactions between *A. Salmonicida* and untreated gut mucins range up to ∼100 nN nm, while interactions with the NeuT gut mucins has a maximum value of ∼1800 nN nm, not shown in the histogram. Values for *Y. Ruckeri* to untreated and treated gut mucins go up to ∼500 and ∼150 nN nm respectively. Treatment with neuraminidase on the gut mucins lead to an increase in deadhesion work for interactions with *A. Salmonicida*, while the same treatment lead to a decrease in work performed for interactions with *Y. Ruckeri*. Even though some interactions had higher deadhesion work, all of the interactions showed a peak for values around 0-50 nN nm, with varying frequency.

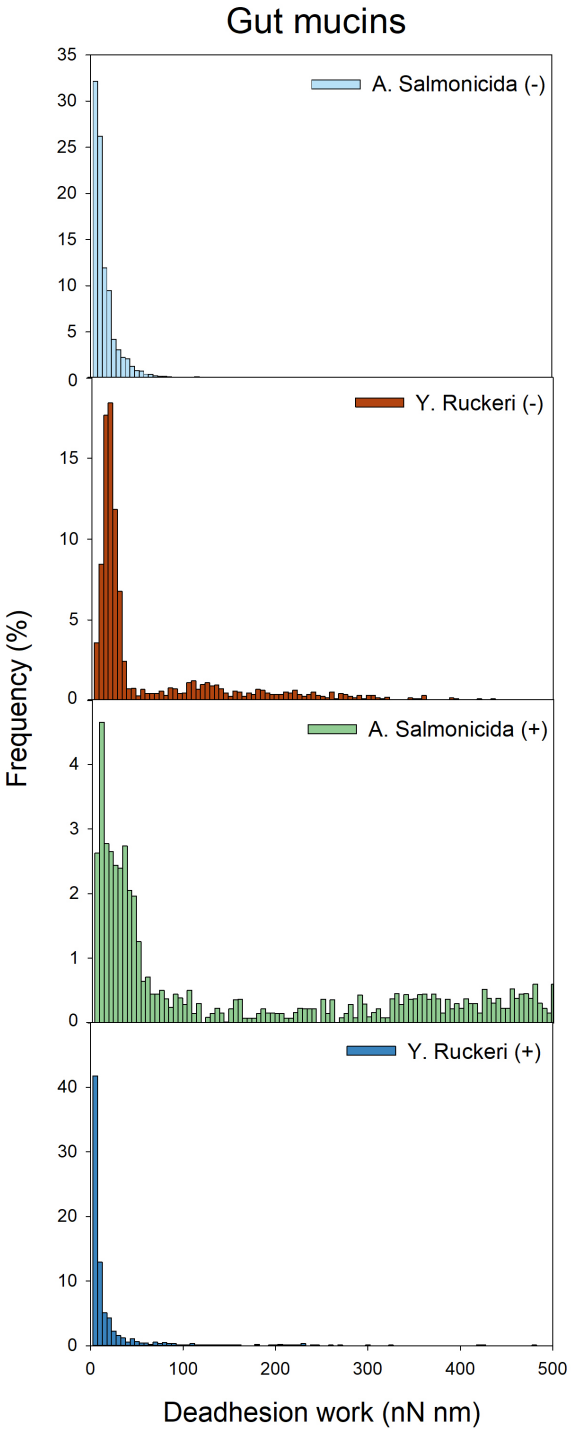

Figure 3.16: Distribution of work performed on molecular interactions between *A. Salmonicida* or *Y. Ruckeri* to Atlantic salmon gut mucins with(+) or without(-) neuraminidase treatment. The histograms portray the distribution of deadhesion work for the different interactions recorded with AFM force spectroscopy. The deadhesion work presented is the total of the three parallels, with modifications done to the frequency of the deadhesion work. The x-axis reaches 600 nN nm, not showing interactions between *A. Salmonicida* and NeuT mucins which had values up to ∼1800 nN nm.

3.4.2 Pathogens - skin mucins

The distribution of deadhesion work for *A. Salmonicida* - skin mucin interactions are placed towards lower values, compared to interactions between *Y. Ruckeri* - skin mucin, *Y. Ruckeri* - NeuT skin mucin, and *A. Salmonicida* - NeuT skin mucin, shown in figure 3.17. Work performed on interactions with skin mucins were different for the two bacteria, and the effect of neuraminidase treatment on interactions depended on the bacteria. Neuraminidase treatment on skin mucins had an effect on the interactions with *A. Salmonicida*, increasing the deadhesion work after treatment with neuraminidase. Interactions with *Y. Ruckeri* decreased slightly after neuraminidase treatment. Deadhesion work for interactions between *A. Salmonicida* and untreated skin mucins range up to ∼100 nN nm, while interactions with skin mucins treated with neuraminidase had a maximum value around 1400 nN nm, not shown in the histogram. Values for *Y. Ruckeri* to untreated and treated skin mucins go up to ∼600 nN nm. The different combinations of interactions had different values for deadhesion work, but a peak at 0-20 nN nm was observed for all adhesion pairs.

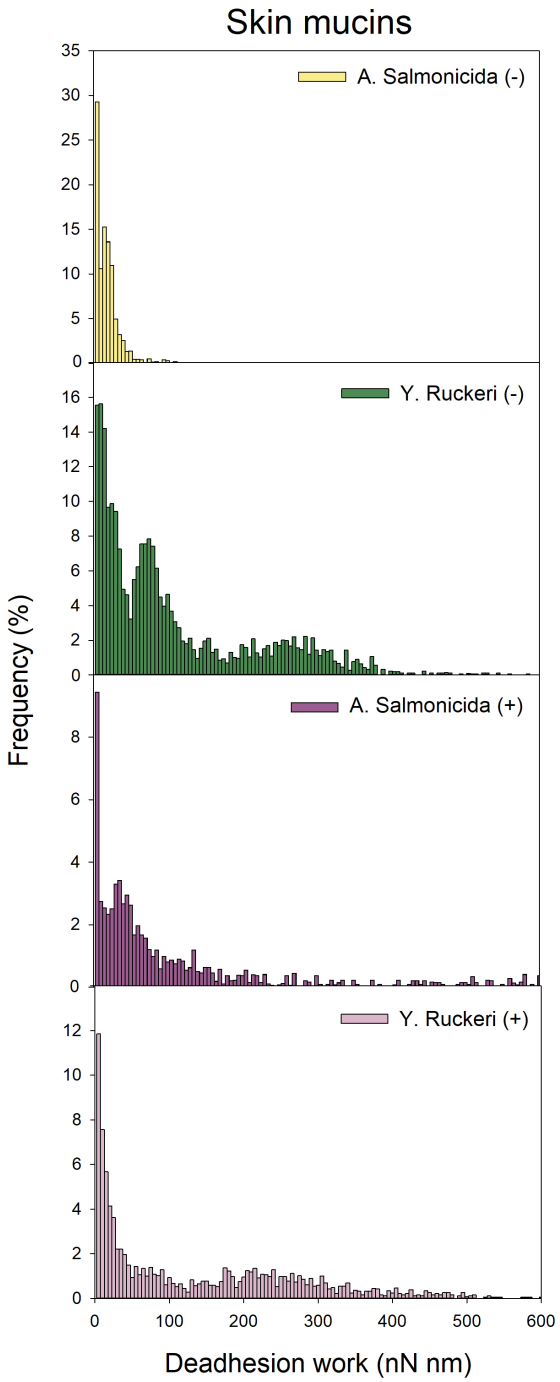

Figure 3.17: Distribution of work performed on molecular interactions between *A. Salmonicida* or *Y. Ruckeri* to Atlantic salmon skin mucins with(+) or without(-) neuraminidase treatment. The histograms portray the distribution of deadhesion work for the different interactions recorded with AFM force spectroscopy. The deadhesion work presented is the total of the three parallels, with modifications done to the frequency of the deadhesion work. The x-axis reaches 600 nN nm, not showing interactions between *A. Salmonicida* and NeuT mucins which had values up to ∼1800 nN nm.

3.5 Heterogenicity

Force-distance curves for each parallel were obtained at three different areas of the mucin coated mica surfaces. A recurring result for the adhesion measurements, was that curves from different areas yielded different values for deadhesion work. Figure 3.18 shows the distribution of deadhesion work for interactions at three different areas of the surface. The deadhesion work displayed were from parallel B of measurements between *Y. Ruckeri* and gut mucins, shown in figure 3.7. Area 1, area 2 and area 3 represent the deadhesion work obtained at these areas, while the total is the sum of the deadhesion work for all areas.

Each area had different values for deadhesion work. Area 1 had a peak at 0-5 nN nm and some interactions with values around 200-300 nN nm were recorded. Area 2 has interactions with deadhesion work ranging from 200-400 nN nm, while area 3 has a strong peak at 100 nN nm. Three peaks are observed in the histogram of the total deadhesion work, and each peak represents results for each area.

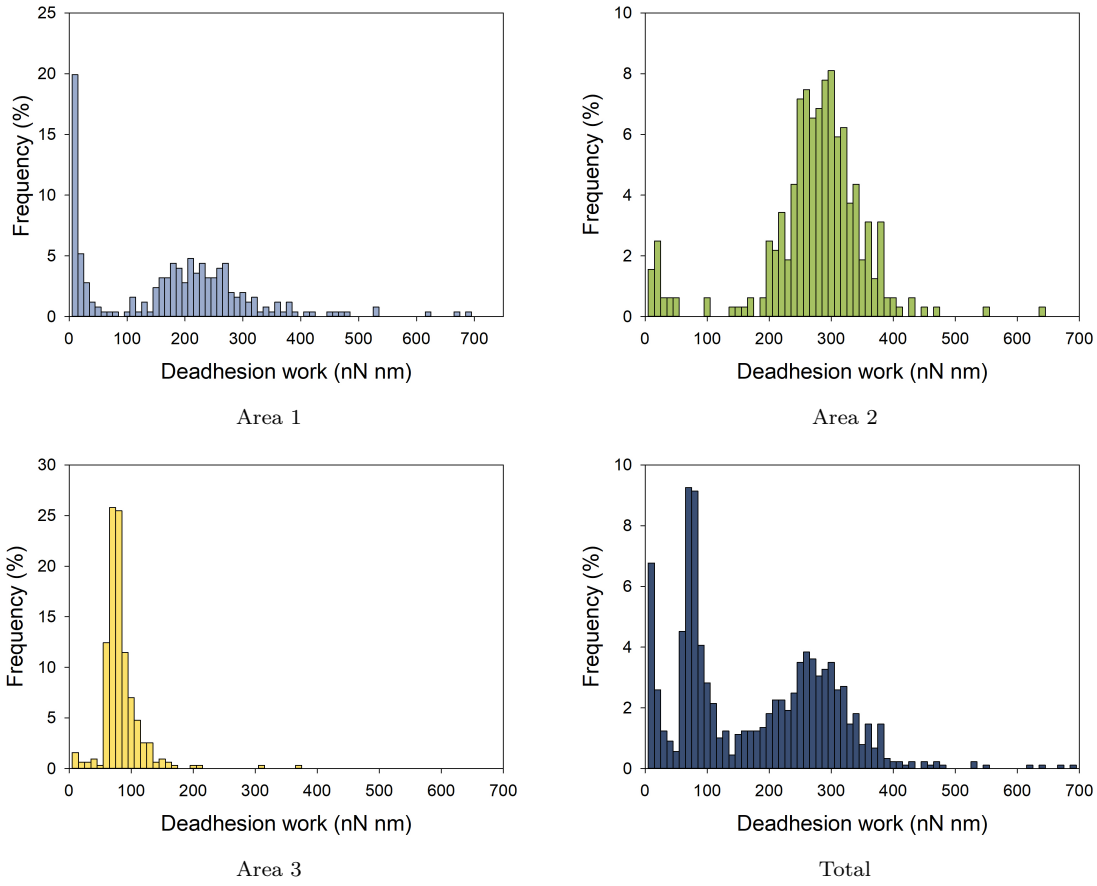

Figure 3.18: Deadhesion work for interactions between *Y. Ruckeri* and Atlantic salmon gut mucins obtained from three different areas of the mucin coated surface. The histograms display the distribution of deadhesion work (nN nm) for the interactions measured by AFM force spectroscopy. Area 1, area 2 and area 3 represent the different areas, and total represents all areas.

3.6 Adhesion of *A. Salmonicida* to skin mucosa of Atlantic salmon

The adhesion of *A. Salmonicida* to the skin mucosa of GF, CVR and CVZ Atlantic salmon fry was investigated by AFM operated in force spectroscopy mode. Three fish of each type were measured. No interactions were recorded for any of the experiments, and there were no observed differences for the results obtained with different types of fish. A selection of force-distance retract curves are presented in figure 3.19

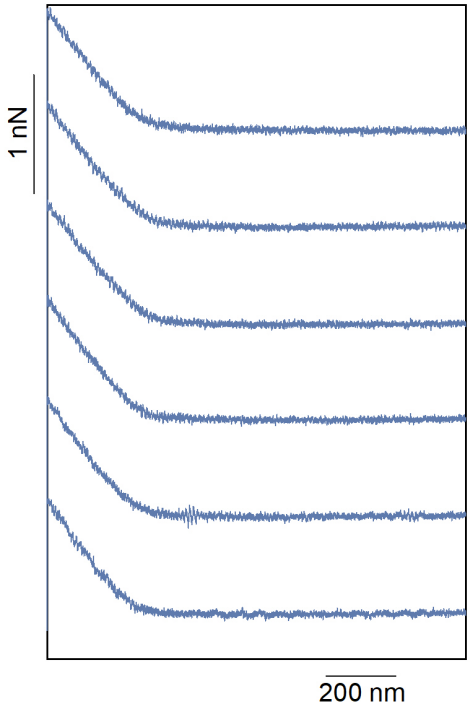

Figure 3.19: A selection of force-distance retract curves from AFM measurements with *A. Salmonicida* and Atlantic salmon fry. The curves are obtained on the skin surface of the fish fry.

Discussion

4.1 Immobilization of bacteria to AFM probes

In order to test bacterial adhesion to mucins using an AFM based approach, the bacteria needed to be chemically attached to the AFM probes. Development of a method that could provide a dense cover of bacteria, which would stay attached and remain viable during experiments were essential to obtain reliable data that represents the actual adhesion interaction.

Two methods were tested and compared to establish an efficient protocol for immobilization of bacteria to AFM probes. The particular methods were based on a procedure developed by former master students Åsa Schawlann Ølnes and Magnhild Sekse Erdal [64, 63]. For their project, they managed to successfully attach the gram-positive *Arthrobacter* sp. and the gram-negative *J. Lividium* to different types of AFM probes (colloidal, triangular and tipless). However, the density of immobilized bacteria was low and the method needed to be modified further to achieve a denser cover of bacteria. The first method used in this thesis was a replica of the protocol developed by the previous team of master students. This is referred to as method 1. As part of this thesis work the method was modified and improved, leading to a new method referred to as method 2. Method 2 is the one used for the AFM measurements. The same bacteria, *Arthrobacter* sp. and *J. Lividium* were used to further develop the findings from the previous master students.

For the two methods tested, the same chemical adherent and the same type of cantilever was utilized. This was based on the results from the previous master students. As part

of their development process, the effect of different adhesive chemicals was compared, including silane-COOH, silane-NH_2 and PDA. The commonly used adhesive polymers PLL or PEI were excluded from the process due to their possible antimicrobial effects [62], which had previously been experienced by members of the research group. The wet adhesive PDA provided the best level of immobilization for both types of bacteria. PDA is a versatile polymer able to form strong bonds in a slightly alkaline, wet environment [65]. As PDA gave the best results, and is acknowledged as an easily applicable and stable chemical, which can immobilize bacteria on a cantilever without affecting cell viability or surface proteins, this chemical was used in the further experimental work [66, 67]. It was decided to use PNP-TR-TL tipless cantilevers as this provided a larger surface for immobilization, in contrast to triangular and colloidal tips where exact positioning of bacteria at the tip was necessary.

The main differences between the two protocols were the centrifugation step and the incubation time after addition of bacteria. Method 1 included two rounds of centrifugation of bacteria, each with a speed of 2000 rpm and a duration equal to 5 minutes. For method 2, the bacteria were added directly from their liquid suspension onto the cantilevers, allowing them to grow directly on the cantilever surface. With the aim of providing optimal growth for bacteria on the cantilever, the centrifugation step was excluded to prevent exposing the bacteria to unnecessary stress. Moreover, a study by Peterson et al. suggested that centrifugation can lead to cell surface damage by exposing the bacterial surface to shear forces caused by collisions between bacteria [68]. In several experimental protocols the effects of centrifugation, other than cell lysis, is assumed to be non-existent. However, the findings from Peterson et al. indicated that centrifugation may affect the cell surface proteins of bacteria. As the surface proteins of bacteria play a vital role in bacterial adhesion to surfaces, such damage may lead to insufficient immobilization of bacteria to cantilevers. It can also influence the adhesion interactions measured by the AFM, and was consequently excluded from the protocol. However, the damage caused by centrifugation depends on the type of bacteria and

increases with increasing centrifugation speed [68, 69]. Despite the increasing use of PDA as a chemical adherent compatible with biomaterials, not much is known about the optimal parameters and the effect such parameters may have on immobilizing biological structures onto PDA coated surfaces. For method 2, the incubation time after addition of bacteria was increased from 20 minutes to overnight. This was done to test the effect of prolonged incubation.

A fluorescence microscopy based live/dead assay was used in order to test the viability and cover of the bacteria immobilized on a tipless cantilever following method 1 and method 2. Method 1 provided a very weak cover of both *Arthrobacter* sp. and *J. Lividium* on the cantilever. The few bacteria observed were positioned near the chip and not on the tip of the cantilever. These results are compatible with the findings from the previous master students, in the sense that there are visible bacteria attached, but the density of immobilized bacteria is insufficient. The suggested modifications of the method leading to method 2 proved to be effective, as the cover of bacteria became denser and the immobilized bacteria were positioned at the tip of the cantilever, as intended. The majority of bacteria were viable after 12 hours. Even though the cover was less dense for *J. Lividium* than *Arthrobacter* sp, it was decided that the density of immobilized bacteria was sufficient for use in the AFM force spectroscopy measurements.

4.1.1 Variability between probes used in experiments with AFM

For the AFM force spectroscopy measurements executed in this thesis, the pathogenic bacteria *A. Salmonicida* and *Y. Ruckeri* were immobilized on tipless cantilevers by method 2. Some probes were stained with live/dead assay and studied in the microscope after use in the AFM. This was done to ensure that there was bacteria immobilized on the tip of the cantilever and that these remained attached and viable for the entire duration of the experiments, which could sometimes last up to 6 hours. Moreover,

images showing the density of immobilized bacteria on cantilevers give important information when interpreting the results obtained from the force spectroscopy experiments.

All the imaged probes had bacteria attached, although the number and position of bacteria varied. The cover of bacteria on the cantilevers ranged from thin to dense, with evenly distributed or clustered bacteria, for both *A. Salmonicida* and *Y. Ruckeri*. It has previously been demonstrated that different types of bacteria can respond differently to the same adhesive chemical [62]. The two bacteria used in the experiments presented in this thesis, *A. Salmonicida* and *Y. Ruckeri*, could thus potentially react differently during immobilization than the ones used during method development, *J. Lividium* and *Arthrobacter*. However, in these experiments the occasional low density does not appear to be caused by the type of bacteria. Instead it seems like the developed method is capable of providing a dense cover of both the gram-negative bacteria, but the large variation between probes show that the method does not produce reliable and reproducible results. In the future, the method for immobilizing bacteria to cantilevers should be improved, with the aim to produce a denser cover with evenly distributed bacteria and low variation between probes. Alternatively, SCFS could be used to avoid the issue with varying density.

The density and position of the bacteria influenced the AFM force spectroscopy measurements. Probes with higher amounts of bacteria located on the tip of the cantilever, such as the probes used in parallel B with *Y. Ruckeri* - NeuT mucins and parallel B with *A. Salmonicida* - NeuT mucins, lead to higher deadhesion work and multiple rupture events. In comparison, probes used in parallel A with *Y. Ruckeri* - NeuT mucins and parallel C with *A. Salmonicida* - NeuT mucins, had fewer bacteria immobilized on the tip, and these experiments gave very low values for deadhesion work and small, mostly individual rupture events. Unfortunately, not all the probes were imaged after use. The large variation in the cover of bacteria was not expected, and the need for images of the probes was discovered late in the work with this master thesis. The varying data for deadhesion work obtained after experiments lead to the suggestion that the

cover of bacteria was not consistent for all probes, which was confirmed by imaging probes after use in the AFM. Without an image of the probe, it is hard to conclude if the weak interactions recorded in some experimental series were a result of the actual interaction between the bacteria and mucin being weak or if it is a consequence of the probe lacking bacteria on the tip. Furthermore, the results for deadhesion work often varied greatly between replicates of one adhesion pair, which is likely a consequence of the inconsistent cover of bacteria. Documentation concerning the density of bacteria on the probes would have been useful for the data interpretation.

4.2 Adhesion strength between pathogenic bacteria and Atlantic salmon mucins

The adhesion of the two pathogens *A. Salmonicida* and *Y. Ruckeri* to Atlantic salmon gut (proximal intestine) and skin mucins was investigated by the use of AFM operated in force spectroscopy mode. The aim of the experiments was to examine the underlying molecular mechanism and forces driving the attachment of these bacteria to mucosal surfaces of Atlantic salmon. It is assumed that bacteria bind mainly to mucins in the mucosa, and specifically the glycan part of mucins. Even though isolated mucins cannot fully reflect the real properties of mucins in their natural environment, it can provide useful information about the adhesive abilities of the pathogens to the tissue-specific glycans of mucins. This can shed light on the preferred attachment site of *A. Salmonicida* and *Y. Ruckeri*, which is quite important for the virulence of the bacteria.

4.2.1 Comparison of pathogenic adhesion strength to skin and gut mucins

The amount of work required to break the interactions between *A. Salmonicida* and Atlantic salmon mucins were found to be relatively low. The majority of deadhesion work performed were in the range of 0 to 60 nN nm, indicating that the interactions

were weak. No differences were observed for the two types of mucins, suggesting that *A. Salmonicida* adhere with similar strength to both gut and skin mucins. These findings differ from the findings presented in a previous study by Padra et al. which concludes that *A. Salmonicida* binds to intestinal mucins to a greater extent than to skin mucins [40]. Such varying results may occur due to the differences in the methods used. For their experiment a microtiter based assay was used, where the binding of bacteria to mucins could take place over a time span of 2 hours, whereas experiments executed in this thesis includes less than a second contact time between the bacteria and mucins. The intestine have also been suggested as a possible entryway by Jutfelt et al. and Ringø et al. [70, 46]. The study executed by Ringø et al. show that *A. Salmonicida* release toxins and enzymes to successfully infect the host. Such mechanisms may be a way for the bacteria to promote adhesion, although these processes occur over time and will not influence the AFM experiments due to its quick contact time. This demonstrates that the AFM measurements cannot show the full extent of the adhesive properties of a bacteria due to the various mechanisms the bacteria can utilize to gain entry to a host. Nevertheless, findings from this thesis can provide information regarding the initial adhesion events occurring between the bacteria and mucins. The results indicate that *A. Salmonicida* does not form stronger attachments to gut mucins than skin mucins, and the low adhesion could suggest that the gut and skin mucosa are not the entryway of *A. Salmonicida* to Atlantic salmon. Another possible route of infection may be the gills, although this has not been looked into in this study [71].

The low values for deadhesion work obtained in measurements with *A. Salmonicida* may be a result of few immobilized bacteria on the AFM cantilever. The AFM probe used in parallel C in these measurements had bacteria attached to the tip, although the quantity was very small. The values of deadhesion work measured in this parallel were very low, which could be a result of a low number of bacteria located on the tip and thus being able to interact with the mucins. No images were obtained from the other experiments with this adhesion pair, although the values of deadhesion work were in the same range.

Due to the lack of images from these experiments it is hard to conclude if the observed low adhesion was a consequence of a low density of immobilized bacteria or if it is an accurate representation of the interactions with skin and gut mucins being indeed weak. The percentage of curves containing interactions can give additional information, seeing as a low percentage can be caused by few bacteria immobilized on the probe. The percentages for parallel C were 70.1% and 47.3% which correlates with the low amount of bacteria on the probe. Values from parallel A showed a high variation with 42.5% for interactions with gut and 93.2% for interactions with skin, which provides little information of the cover of bacteria. Parallel B showed a consistently high percentage which could indicate that there was a dense cover of bacteria on the probe used.

The frequent variation in deadhesion work and interaction probability can be caused by other factors than the density of bacteria on the probe. Biological surfaces are of a heterogeneous nature. Bacteria have a diverse cover of molecules, including various lipids, surface proteins and adhesins that have been shown to form clusters on bacterial surfaces to promote adhesion through multivalency [72]. This can give rise to different ways for the bacteria to interact with the sample, depending on the specific molecules positioned to interact with the sample. Additionally, the mucin sample provides a cover of glycans, that can consist of a varying amount and different types of oligosaccharides [15, 73]. As the AFM force spectroscopy measurements are operated on a very small area, the distribution of glycans may influence the deadhesion work measured. The position of the glycans, and the terminal structures present in this specific area, may lead to various amounts of interactions occurring at different areas. Results obtained from measurements at three different areas with the same probe and mucin sample are shown in section 3.5, where the deadhesion work varies for each area. This could be a result of a varying distribution of adhesion molecules on the bacterial surface, or the distribution of glycans on the sample surface.

The deadhesion work was higher for interactions between *Y. Ruckeri* and skin mucins, than *Y. Ruckeri* and gut mucins. This deviates from previous findings, which suggest

that gut and gills are the preferred entryway of *Y. Ruckeri* [50, 51]. Nonetheless, little is known about the pathogenic mechanisms the bacteria use to overcome host defenses, so the skin may be a possible route. It has been hypothesized that *Y. Ruckeri* express pili, due to its high adhesion to surfaces. If the skin is the infection route of *Y. Ruckeri*, the expression of pili would be highly advantegous due to its ability to widthstand high shear forces caused by the rinsing flows of water. The results suggest that *Y. Ruckeri* can bind more strongly to Atlantic salmon mucins, especially skin mucins, than *A. Salmonicida*. This differs from the findings presented by Padra et al. showing that *A. Salmonicida* bound better to mucins than *Y. Ruckeri*, and that gut mucins had the highest binding avidity for both bacteria [6]. However, as previously mentioned, these findings may be a result of the different methods used, as their experiments used a microtiter-based assay.

The results from experiments with *Y. Ruckeri* varied between replicates. Results from parallel A and B showed a similar trend as interactions with skin had higher values for deadhesion work than interactions with gut. Parallel C had high values for interactions with both skin and gut, and the probe used in this parallel was the only probe from the three parallels that was imaged after use. The image showed a cluster of bacteria positioned at the tip of the cantilever, indicating that the measured deadhesion work represents interactions between the bacteria in this cluster and mucins. Despite this, the results from A and B were emphasized as they both showed the same trend, and the percentage of curves containing interactions were quite high for all replicates, suggesting that there was a sufficient cover of bacteria on all the probes.

4.2.2 Binding types and rupture forces for interactions between pathogens and mucins

The binding type cannot be accurately determined for the interactions obtained in this thesis. However, comparison with curves showing specific interaction types and values for binding strength obtained in other studies can offer some indication of the binding

mechanism.

The majority of recorded interactions were clearly specific forces arising from ligand-receptor interactions. Force curves obtained from measurements with *A. Salmonicida* had small, single or multiple rupture events. The force curves obtained from measurements with *Y. Ruckeri*, were similar to those acquired with *A. Salmonicida*, although some of the interactions with *Y. Ruckeri* were larger and had a higher amount of multiple rupture events. The features of these rupture events were quite similar to rupture events for ligand binding of specific adhesins, shown in figure 1.9A. This represents binding of specific adhesins, that undergo conformational changes to bind and create a stable adhesin-ligand complex [74]. Despite the similarity between rupture events, the rupture forces of such bonds were measured to be quite strong, up to $\sim$2 nN. This is a great deal higher than the rupture forces recorded for interactions between the pathogens and mucins, which were around 0.2 nN. The force curves obtained from interactions with the pathogens and mucins also share similarities with force curves showing carbohydrate-lectin binding obtained from measurements of a single *Lactobacillus plantarum* bacterium and lectins [75]. These recorded interactions had weaker rupture forces, around 0.25 nN, similar to the forces measured for *A. Salmonicida* and *Y. Ruckeri*. The similarities between force curves recorded for the two bacteria may indicate that both types of bacteria adhere to the mucosal surfaces through a low number of weak intermolecular interactions, such as lectin-carbohydrate bonds. Additionally, some of the retract curves had rupture events occurring after the probe had been retracted more than 400 nm. This could indicate that pili structures are involved, as such long rupture distances could be caused by an extension of pili, or alternatively by the extension of mucins.

The rupture forces for interactions between the pathogens, *A. Salmonicida* or *Y. Ruckeri*, and the Atlantic salmon mucins were fairly similar for all adhesion pairs. A large proportion of the rupture forces ranged from 0.1-0.3 nN, which are relatively weak interactions. The rupture force increased with an increasing loading rate, that ranged

from 10-100 nN/s. Other studies have shown similar low rupture forces for lectin-glycan interactions with bacteria. Le et al. found that a single *Lactococcus lactis* bacterium bound to mucins with a strength of approximately 0.08-0.12 nN [76]. As previously mentioned, glycans on *L. plantarum* were found to bind to glucose-specific lectins with the force of 0.25 nN [75]. Results from SMFS experiments measuring glycan-lectin binding, or glycan-glycan binding, showed a similar trend of relatively weak interactions. Sletmoen et al. measured forces from 0.2-0.3 nN for interactions between a modified porcine submaxillary mucin (Tn-PSM), containing only α-linked GalNAc residues, and GalNAc-specific lectins [77]. Interactions between SpaC, the adhesion protein of a pili, and mucins had forces between 0.07-0.09 nN [78]. Glycan-glycan interactions recorded from Tn-PSM self-interactions were found to have a force of approximately 0.05-0.1 nN [79]. This shows that the typical interactions that may occur between a bacteria and mucins are generally weaker, which corresponds with the findings in this study. The weakness of the adhesion forces may benefit the bacteria, by allowing its escape from sites where bacterial host defenses are most vigorous, such as the mucosal surfaces. Interestingly some studies with bacteria-cell interactions have shown stronger forces. A strain of *Staphylococcus aureus* were found to bind to proteins found in the extracellular matrix with a strength of 1-2 nN, and Liu et al. showed that a strain of fimbriated *E. coli* bound to cells with up to 9 nN [72, 80]. The difference in strength between bacteria-mucins and bacteria-cells can suggest that the weak binding force may be a result of the protective properties of mucus. As the mucus functions as a barrier between the exterior and the host, its main purpose is to shut out harmful organisms, and the low interaction force may be a way to do this.

Due to the possibility of multiple binding interactions, it is hard to draw any conclusion regarding the binding mechanisms utilized by the bacteria from the rupture forces and features of the rupture events. A high rupture force could be a result of one strong interaction, or the result of several weak interactions. As the cantilevers used in the experiments have multiple bacteria attached, several bacteria can interact with the

sample at once. The rupture forces were decided for only one parallel of experiments, instead of all three. As the data for the three replicates varied, analysis from one parallel does not show the full extent of the rupture forces. Additionally, several rupture events were excluded due to the high multiplicity of the interaction, which could lead to exclusion of typical curves from interactions between specific adhesins, MUB and pili. Consequently, the values obtained for rupture forces does not represent the full extent of interactions.

4.3 The effect of sialic acids in pathogenic adhesion

The adhesion of the two pathogens *A. Salmonicida* and *Y. Ruckeri* to NeuT Atlantic salmon mucins were investigated by the use of AFM force spectroscopy. Sialic acids are common terminal structures that have various functions in bacterial adhesion. The negatively charged molecule can either mask underlying recognition sites or function as a recognition site itself. Due to its importance in bacterial adhesion, and the high content of sialic acids on Atlantic salmon mucins [40, 5], it was hypothesized that sialic acids influence the adhesion of the two salmonid pathogens *A. Salmonicida* and *Y. Ruckeri* to Atlantic salmon. Neuraminidase was used to remove sialic acids, and the adhesion of the bacteria to mucins, both with and without sialic acids, was compared.

For the experiments executed with NeuT mucins, the results varied strongly between parallels. Fortunately, the majority of probes used in these measurements were imaged after use, thus providing valuable information regarding the amount of bacteria. Figures 3.16 and 3.17 have collected data from the three parallels of each adhesion pair to compare the results with and without neuraminidase treatment. Modifications were made to the frequency of observations to prevent some peaks from becoming more prominent. For experiments with NeuT mucins, the parallel with a dense cover of bacteria was emphasized in these figures. This was parallel B for experiments using an *Y. Ruckeri* covered probe. No image was obtained of the probe used in parallel A of

experiments with *A. Salmonicida*, although images from B and C showed that B had a slightly denser cover so results from this measurement was prioritized.

The amount of work required to break the interactions between *A. Salmonicida* and Atlantic salmon mucins, increased with neuraminidase treatment. This suggests that the terminal sialic acids masks underlying recognition sites on the mucins, and that *A. Salmonicida* does not contain sialic acid-specific lectins. This contradicts the findings of Padra et al. which showed that sialic acids promoted the adhesion of *A. Salmonicida* [40]. Nevertheless, our findings indicate that *A. Salmonicida* cannot bind to sialic acids, and the adhesion strategy must involve binding to other types of carbohydrates. As *A. Salmonicida* commonly infect Atlantic salmon, which contain mucins that are frequently terminated with sialic acids, other mechanisms can be involved in mediating the attachment of the bacteria. In vivo, the mucosal microbiota can contain bacteria able to cleave sialic acids, providing binding sites for *A. Salmonicida*, as well as access to underlying carbohydrates it can catabolize.

The results showed that *A. Salmonicida* bound better to NeuT gut mucins than NeuT skin mucins. This correlates well with the results found by Padra et al. suggesting that the intestine has a higher level of sialylation than the skin [40]. Additionally, it has been found that the skin mucosa has a different flora and considerably lower bacterial counts than the intestine [81]. This could lead to a higher amount of bacteria cleaving off the sialic acids in the gut, possibly resulting in *A. Salmonicida* being better adapted to attach to the underlying sites of sialic acids in this area. Furthermore, it has been found that GlcNAc is the only glycan structure present terminally on the salmon mucins that enhances growth of *A. Salmonicida* [5]. This study also found that GlcNAc was the second most abundant terminal residue in the gut, and was less frequently found on terminal sites in the skin. As binding to this area could provide better growth for *A. Salmonicida* it could have adapted specific lectins for this carbohydrate, although this is not known. The high sialic acid content of the gut mucins provides a high negative charge that could shield this potential binding site. By removing this dense negative

charge the pathogen could gain access to these terminal structures.

Neuraminidase treatment lead to a decrease in deadhesion work for interactions between *Y. Ruckeri* and Atlantic salmon mucins. The decrease in binding could indicate that *Y. Ruckeri* have sialic acid-specific lectins, and that removing sialic acids eliminates important binding sites for the pathogen. The change in deadhesion work was more prominent for interactions with gut than skin. This could be a result of gut having a higher content of sialic acids, and removing these binding sites would thus have a larger impact on the adhesion to gut than skin. However, it is worth mentioning that two of the parallels for interactions between *Y. Ruckeri* and untreated mucins had very low binding with gut, which makes the effect of sialic acids in the binding process more uncertain. For interactions between *Y. Ruckeri* and skin it may be possible that the pathogen binds more frequently to other terminal residues than sialic acids, as high values for deadhesion work was still detected after the neuraminidase treatment.

The rupture forces were similar for interactions with the pathogens and untreated or NeuT mucins. The forces were relatively low, although a small increase in the forces between *A. Salmonicida* and NeuT mucins was observed. The increase in rupture forces is likely due to the increase in binding sites for *A. Salmonicida* on the NeuT mucins, which could lead to multiple bonds forming, requiring higher rupture forces to break them apart. The characteristics of the force curves obtained from parallel B of experiments with *A. Salmonicida* and NeuT mucins, also differed from measurements with untreated mucins, as they had larger and a higher amount of multiple rupture events, representing these multiple bonds.

4.4 Adhesion of *A. Salmonicida* to Atlantic salmon skin mucosa

The adhesion of *A. Salmonicida* to the skin mucosa of GF, CVR and CVZ Atlantic salmon fry was investigated by using AFM operated in force spectroscopy mode. These

measurements were executed to study the adhesion mechanism of the pathogen directly to the skin mucus of Atlantic salmon, while also examining the effect gnotobiotic treatment of salmon fry would have on the mucus binding properties. The latter was not possible to investigate as the experiments did not record any interactions for the different fish types. However, the cause for the absence of interactions was investigated.

During the execution of the force spectroscopy experiments with the fish fry, there were difficulties in obtaining proper curves. Due to the soft texture of the sample, finding a contact point was challenging as the tip seemed to slide through the mucus. The AFM measurements became increasingly hard to obtain over time, as the fry became more and more dissolved and covered with secreted mucus. For this reason, several curves had to be discarded and possible interactions were not measured. However, some curves had a specific contact point and were usable, although none of these contained any interactions. Very few viable curves were obtained, making the results less reliable and difficult to obtain a significant conclusion from. However, it can be concluded that the softness of the outer mucus layer of fish skin provides a challenging surface to perform AFM force spectroscopy measurements on.

The previous master students used the same method with different bacteria, and faced the same issues due to the softness of the sample. Nevertheless, they had visible interactions in the viable curves. Thus, the lack of recorded interactions in this thesis is likely a result of no interactions occurring between *A. Salmonicida* and the skin mucus surface. AFM mesurements between *A. Salmonicida* and Atlantic salmon skin mucins, extracted from secreted mucus, provided relatively weak binding, which could indicate that the skin is not the preferred entryway for *A. Salmoncida*. Additionally, the mucins in mucus are bound together in networks, making them harder to bind to. Cuts on the skin surface of Atlantic salmon have been shown to give a distinct increase in the lethality of the pathogen [82]. This may indicate that the skin mucosa is an efficient barrier, and needs to be fully breached for *A. Salmonicida* to penetrate it. However, the bacteria is known to release toxins and enzymes, which could compromise the mucus

barrier by degrading important components of the mucus. The effect the disruption of the mucus layer would have on the adhesion of the bacteria is not known, although it is plausible that such an effect exists.

4.5 Future prospects

The present study showed that the adhesion of the pathogens *A. Salmonicida* and *Y. Ruckeri* to the mucins and skin mucosa of Atlantic salmon is a complex process that needs to be further studied. The use of AFM force measurements provide important information concerning the adhesion of chosen bacteria to fish mucosa, and this information is complementary to the information obtained using alternative and more traditional methods. Still, the data interpretation and the reliability of the method would benefit from further improvement and validation of the method.

Due to the varying density of immobilized bacteria on the cantilever, the method for immobilization should be further developed. As PDA proved to be a successful adhesive chemical, it is recommended for further use. However, the effect of different parameters, such as concentration, incubation time and temperature should be further explored. Additionally, obtaining images of the probes used in experiments should be continued, as it can provide valuable information of interactions obtained from this type of experiment.

Results obtained from measurements with the AFM did not provide sufficient information about the binding mechanisms for the two pathogens to mucins. To get a more detailed understanding of these mechanism, SCFS should be used. By allowing one bacteria to interact with mucins, quantitative data for deadhesion work and rupture forces for a single bacteria can be obtained. This also removes the complications of a varying cover of bacteria.

A disadvantage that occurred when the effect of sialic acids for bacterial adhesion was evaluated, was that different probes had been used and the results were therefore

difficult to compare. To better compare results from experiments, the same probe should be used in these experiments.

Using fish as a sample for AFM measurements also caused some complications. The continued secretion of the viscous mucus membrane made the texture of the sample too soft, resulting in issues with the AFM measurements. A possible solution to this problem could be to use snap-freezing of the fish before use. This could potentially remove the highly viscous outer mucus layer, whilst maintaining the inner mucus layer. In this way, the sample would become firmer without totally removing the mucus layer. Another solution could be to remove some of the secreted mucus, and immobilize it on a harder material. This would create a firmer base, making it easier to obtain a proper contact point.

Conclusion

The aim of this study was to get a better understanding of the adhesion of the pathogens *A. Salmonicida* and *Y. Ruckeri* to the mucosal surfaces of Atlantic salmon.

Results obtained for deadhesion work showed that *A. Salmonicida* bound weakly to both skin and gut mucins, which suggest that the bacteria have difficulties in binding to these mucosal sites in Atlantic salmon. AFM experiments executed with *A. Salmonicida* directly to the skin mucosa of Atlantic salmon fry further confirmed these findings, as no interactions were observed. Results from experiments with the NeuT mucins indicate that the bacteria does not bind to sialic acids, and that these terminal residues masks underlying recognition sites for the bacterium.

AFM experiments with *Y. Ruckeri*, showed that the bacteria bound better to skin mucins than gut mucins. This suggests that the pathogen may have developed improved binding mechanisms for the skin mucosa, and that this could potentially be the preferred route of entry for the bacteria into the fish. Sialic acids were found to be potential binding sites for *Y. Ruckeri*, although other terminal residues were suggested to play important parts in the adhesion of the bacteria.

The rupture forces were relatively weak for both *A. Salmonicida* and *Y. Ruckeri*. This may indicate that the pathogens adhere to the mucosal surface through a low number of weak intermolecular interactions, such as lectin-carbohydrate bonds.

Bibliography

[1] G. Kumar, S. Menanteau-Ledouble, M. Saleh, and M. El-Matbouli. "Yersinia ruckeri, the causative agent of enteric redmouth disease in fish". In: *Veterinary Research* 46.1 (Sept. 2015). DOI: 10.1186/s13567-015-0238-4.

[2] G. Merino, M. Barange, J. L. Blanchard, J. Harle, R. Holmes, I. Allen, E. H. Allison, M. C. Badjeck, N. K. Dulvy, J. Holt, S. Jennings, C. Mullon, and L. D. Rodwell. "Can marine fisheries and aquaculture meet fish demand from a growing human population in a changing climate?" In: *Global Environmental Change* 22.4 (Oct. 2012), pp. 795–806. DOI: 10.1016/j.gloenvcha.2012.03.003.

[3] E. Tobback, A. Decostere, K. Hermans, F. Haesebrouck, and K. Chiers. "Yersinia ruckeri infections in salmonid fish". In: *Journal of Fish Diseases* 30.5 (May 2007), pp. 257–268. DOI: 10.1111/j.1365-2761.2007.00816.x.

[4] S. Dallaire-Dufresne, K. H. Tanaka, M. V. Trudel, A. Lafaille, and S. J. Charette. "Virulence, genomic features, and plasticity of Aeromonas salmonicida subsp. salmonicida, the causative agent of fish furunculosis". In: *Veterinary Microbiology* 169.1-2 (Feb. 2014), pp. 1–7. DOI: 10.1016/j.vetmic.2013.06.025.

[5] J. T. Padra, H. Sundh, K. Sundell, V. Venkatakrishnan, C. Jin, T. Samuelsson, N. G. Karlsson, and S. K. Lindén. "*Aeromonas salmonicida* Growth in Response to Atlantic Salmon Mucins Differs between Epithelial Sites, Is Governed by Sialylated and N-Acetylhexosamine-Containing O-Glycans, and Is Affected by Ca2+". In: *Infection and Immunity* 85.8 (2017). Ed. by B. McCormick. ISSN: 0019-9567. DOI: 10.1128/IAI.00189-17.

[6] J. T. Padra, A. V. M. Murugan, K. Sundell, H. Sundh, J. Benktander, and S. K. Linden. "Fish pathogen binding to mucins from Atlantic salmon and Arctic char differs in avidity and specificity and is modulated by fluid velocity". In: *PLOS ONE* 14.5 (May 2019), pp. 1–18. DOI: 10.1371/journal.pone.0215583.

[7] Ł. Grześkowiak, M. C. Collado, S. Vesterlund, J. Mazurkiewicz, and S. Salminen. "Adhesion abilities of commensal fish bacteria by use of mucus model system: Quantitative analysis". In: *Aquaculture* 318.1-2 (July 2011), pp. 33–36. DOI: 10.1016/j.aquaculture.2011.04.037.

[8] C. Jin, J. T. Padra, K. Sundell, H. Sundh, N. G. Karlsson, and S. K. Lindén. "Atlantic Salmon Carries a Range of Novel O-Glycan Structures Differentially Localized on Skin and Intestinal Mucins". In: *Journal of Proteome Research* 14.8 (June 2015), pp. 3239–3251. DOI: 10.1021/acs.jproteome.5b00232.

[9] I. Salinas. "The Mucosal Immune System of Teleost Fish". In: *Biology* 4.3 (Aug. 2015), pp. 525–539. DOI: 10.3390/biology4030525.

[10] C. Formosa-Dague, M. Castelain, H. Martin-Yken, K. Dunker, E. Dague, and M. Sletmoen. "The Role of Glycans in Bacterial Adhesion to Mucosal Surfaces: How Can Single-Molecule Techniques Advance Our Understanding?" In: *Microorganisms* 6.2 (May 2018), p. 39. DOI: 10.3390/microorganisms6020039.

[11] J. Cai, ed. *Atomic Force Microscopy in Molecular and Cell Biology*. eng. Singapore, 2018.

[12] *Bacterial Adhesion: Chemistry, Biology and Physics*. eng. Vol. 715. Advances in Experimental Medicine and Biology. Dordrecht: Springer Netherlands, 2011. ISBN: 9789400709393.

[13] O. Axner, O. Björnham, M. Castelain, E. Koutris, S. Schedin, E. Fällman, and M. Andersson. "Unraveling the Secrets of Bacterial Adhesion Organelles Using Single-Molecule Force Spectroscopy". In: *Single Molecule Spectroscopy in Chemistry, Physics and Biology*. Springer Berlin Heidelberg, Nov. 2009, pp. 337–362. DOI: 10.1007/978-3-642-02597-6_18.

[14] H. J. Busscher, W. Norde, and H. C. van der Mei. "Specific Molecular Recognition and Nonspecific Contributions to Bacterial Interaction Forces". In: *Applied and Environmental Microbiology* 74.9 (Mar. 2008), pp. 2559–2564. DOI: 10.1128/aem.02839-07.

[15] S. K. Linden, P. Sutton, N. G. Karlsson, V. Korolik, and M. A. McGuckin. "Mucins in the mucosal barrier to infection". In: *Mucosal Immunology* 1.3 (Mar. 2008), pp. 183–197. DOI: 10.1038/mi.2008.5.

[16] V. Nizet, A. Varki, and M. Aebi. *Microbial Lectins: Hemagglutinins, Adhesins, and Toxins*. Ed. by V. A. C. R. E. J. et al. 3rd ed. Cold Spring Harbor (NYC): Cold Spring Harbor Laboratory Press; 2015-2017, 2017. Chap. 37. DOI: 10.1101/glycobiology.3e.037.

[17] D. L. Nelson and M. M. Cox. *Principles of Biochemistry*. 6th ed. New York: W. H. Freeman and Company, 2013. ISBN: 9781464109621.

[18] C. R. Epler Barbercheck, E. Bullitt, and M. Andersson. "Bacterial Adhesion Pili". In: *Membrane Protein Complexes: Structure and Function*. Ed. by J. R. Harris and E. J. Boekema. Singapore: Springer Singapore, 2018, pp. 1–18. ISBN: 978-981-10-7757-9. DOI: 10.1007/978-981-10-7757-9_1.

[19] J.-F. Sicard, G. L. Bihan, P. Vogeleer, M. Jacques, and J. Harel. "Interactions of Intestinal Bacteria with Components of the Intestinal Mucus". In: *Frontiers in Cellular and Infection Microbiology* 7 (Sept. 2017). DOI: 10.3389/fcimb.2017.00387.

[20] J. Boekhorst, Q. Helmer, M. Kleerebezem, and R. J. Siezen. "Comparative analysis of proteins with a mucus-binding domain found exclusively in lactic acid bacteria". In: *Microbiology* 152.1 (Jan. 2006), pp. 273–280. DOI: 10.1099/mic.0.28415-0.

[21] I. Belotserkovsky, K. Brunner, L. Pinaud, A. Rouvinski, M. Dellarole, B. Baron, G. Dubey, F. Samassa, C. Parsot, P. Sansonetti, and A. Phalipon. "Glycan-Glycan Interaction Determines Shigella Tropism toward Human T Lymphocytes". In: *mBio* 9.1 (Feb. 2018). Ed. by V. J. Torres. DOI: 10.1128/mbio.02309-17.

[22] S. D. Carrington, M. Clyne, C. J. Reid, E. FitzPatrick, and A. P. Corfield. "Chapter 33 - Microbial interaction with mucus and mucins". In: *Microbial Glycobiology*. Ed. by O. Holst, P. J. Brennan, M. von Itzstein, and A. P. Moran. San Diego: Academic Press, 2010, pp. 655–671. ISBN: 978-0-12-374546-0. DOI: https://doi.org/10.1016/B978-0-12-374546-0.00033-X.

[23] R. Bansil and B. S. Turner. "Mucin structure, aggregation, physiological functions and biomedical applications". In: *Current Opinion in Colloid & Interface Science* 11.2-3 (June 2006), pp. 164–170. DOI: 10.1016/j.cocis.2005.11.001.

[24] R. Bansil and B. S. Turner. "The biology of mucus: Composition, synthesis and organization". In: *Advanced Drug Delivery Reviews* 124 (Jan. 2018), pp. 3–15. DOI: 10.1016/j.addr.2017.09.023.

[25] S. S. Dhanisha, C. Guruvayoorappan, S. Drishya, and P. Abeesh. "Mucins: Structural diversity, biosynthesis, its role in pathogenesis and as possible therapeutic targets". In:

Critical Reviews in Oncology/Hematology 122 (2018), pp. 98–122. ISSN: 1040-8428. DOI: https://doi.org/10.1016/j.critrevonc.2017.12.006.

[26] A. P. Corfield. "Mucins: A biologically relevant glycan barrier in mucosal protection". In: *Biochimica et Biophysica Acta (BBA) - General Subjects* 1850.1 (2015), pp. 236–252. ISSN: 0304-4165. DOI: https://doi.org/10.1016/j.bbagen.2014.05.003.

[27] I. Brockhausen and P. Stanley. *O-GalNAc Glycans*. Ed. by V. A. C. R. E. J. et al. 3rd ed. Cold Spring Harbor (NYC): Cold Spring Harbor Laboratory Press; 2015-2017, 2017. Chap. 10. DOI: 10.1101/glycobiology.3e.010.

[28] E. R. Vimr. "Unified Theory of Bacterial Sialometabolism: How and Why Bacteria Metabolize Host Sialic Acids". In: *ISRN Microbiology* 2013 (2013), pp. 1–26. DOI: 10.1155/2013/816713.

[29] A. Varki, R. Schnaar, and R. Schauer. *Sialic Acids and Other Nonulosonic Acids*. Ed. by V. A. C. R. E. J. et al. 3rd ed. Cold Spring Harbor (NYC): Cold Spring Harbor Laboratory Press; 2015-2017, 2017. Chap. 15. DOI: 10.1101/glycobiology.3e.015.

[30] A. Varki. "Sialic acids as ligands in recognition phenomena." In: *The FASEB Journal* 11.4 (1997). PMID: 9068613, pp. 248–255. DOI: 10.1096/fasebj.11.4.9068613.

[31] C. Traving and R. Schauer. "Structure, function and metabolism of sialic acids". In: *Cellular and Molecular Life Sciences CMLS* 54.12 (Dec. 1998), pp. 1330–1349. DOI: 10.1007/s000180050258.

[32] R. Schauer. "Sialic acids and their role as biological masks". In: *Trends in Biochemical Sciences* 10.9 (Sept. 1985), pp. 357–360. DOI: 10.1016/0968-0004(85)90112-4.

[33] X. Chen and A. Varki. "Advances in the Biology and Chemistry of Sialic Acids". In: *ACS Chemical Biology* 5.2 (Jan. 2010), pp. 163–176. DOI: 10.1021/cb900266r.

[34] T. Miyagi and K. Yamaguchi. "Mammalian sialidases: Physiological and pathological roles in cellular functions". In: *Glycobiology* 22.7 (Feb. 2012), pp. 880–896. DOI: 10.1093/glycob/cws057.

[35] A. L. Lewis and W. G. Lewis. "Host sialoglycans and bacterial sialidases: a mucosal perspective". In: *Cellular Microbiology* 14.8 (May 2012), pp. 1174–1182. DOI: 10.1111/j.1462-5822.2012.01807.x.

[36] M. Ãngeles Esteban. "An Overview of the Immunological Defenses in Fish Skin". eng. In: *ISRN immunology* 2012 (2012), pp. 1–29. ISSN: 2090-5653.

[37] T. Forseth, B. T. Barlaup, B. Finstad, P. Fiske, H. Gjøsæter, M. Falkegård, A. Hindar, T. A. Mo, A. H. Rikardsen, E. B. Thorstad, L. A. Vøllestad, and V. Wennevik. "The major threats to Atlantic salmon in Norway". In: *ICES Journal of Marine Science* 74.6 (Mar. 2017). Ed. by M. Gibbs, pp. 1496–1513. DOI: 10.1093/icesjms/fsx020.

[38] "The Atlantic salmon; genetics, conservation and management". eng. In: *SciTech Book News* 32.1 (2008). ISSN: 0196-6006.

[39] G. Micallef, R. Bickerdike, C. Reiff, J. M. O. Fernandes, A. S. Bowman, and S. A. M. Martin. "Exploring the Transcriptome of Atlantic Salmon (Salmo salar) Skin, a Major Defense Organ". In: *Marine Biotechnology* 14.5 (Apr. 2012), pp. 559–569. DOI: 10.1007/s10126-012-9447-2.

[40] J. T. Padra, H. Sundh, C. Jin, N. G. Karlsson, K. Sundell, and S. K. Lindén. "Aeromonas salmonicida Binds Differentially to Mucins Isolated from Skin and Intestinal Regions of Atlantic Salmon in an N-Acetylneuraminic Acid-Dependent Manner". In: *Infection and Immunity* 82.12 (2014). Ed. by B. A. McCormick, pp. 5235–5245. ISSN: 0019-9567. DOI: 10.1128/IAI.01931-14.

[41] M. Soto-Dávila, A. Hossain, S. Chakraborty, M. L. Rise, and J. Santander. "Aeromonas salmonicida subsp. salmonicida Early Infection and Immune Response of Atlantic Cod (Gadus morhua L.) Primary Macrophages". In: *Frontiers in Immunology* 10 (June 2019). DOI: 10.3389/fimmu.2019.01237.

[42] R. Beaz-Hidalgo and M. J. Figueras. "Aeromonasspp. whole genomes and virulence factors implicated in fish disease". In: *Journal of Fish Diseases* 36.4 (Jan. 2013), pp. 371–388. DOI: 10.1111/jfd.12025.

[43] A. Dacanay, J. Boyd, M. Fast, L. Knickle, and M. Reith. "Aeromonas salmonicida Type I pilus system contributes to host colonization but not invasion". In: *Diseases of Aquatic Organisms* 88 (Feb. 2010), pp. 199–206. DOI: 10.3354/dao02157.

[44] J. M. Boyd, A. Dacanay, L. C. Knickle, A. Touhami, L. L. Brown, M. H. Jericho, S. C. Johnson, and M. Reith. "Contribution of Type IV Pili to the Virulence of Aeromonas salmonicida subsp. salmonicida in Atlantic Salmon (Salmo salar L.)" In: *Infection and Immunity* 76.4 (Jan. 2008), pp. 1445–1455. DOI: 10.1128/iai.01019-07.

[45] K. Valderrama, M. Soto-Dávila, C. Segovia, I. Vásquez, M. Dang, and J. Santander. "Aeromonas salmonicida infects Atlantic salmon (Salmo salar) erythrocytes". In: *Journal of Fish Diseases* 42.11 (Aug. 2019), pp. 1601–1608. DOI: 10.1111/jfd.13077.

[46] E. Ringø, F. Jutfelt, P. Kanapathippillai, Y. Bakken, K. Sundell, J. Glette, T. M. Mayhew, R. Myklebust, and R. E. Olsen. "Damaging effect of the fish pathogen Aeromonas salmonicida ssp. salmonicida on intestinal enterocytes of Atlantic salmon (Salmo salar L.)" In: *Cell and Tissue Research* 318.2 (Aug. 2004), pp. 305–311. DOI: 10.1007/s00441-004-0934-2.

[47] A. Wrobel, C. Ottoni, J. C. Leo, S. Gulla, and D. Linke. "The repeat structure of two paralogous genes, Yersinia ruckeri invasin (yrInv) and a "Y. ruckeri invasin-like molecule", (yrIlm) sheds light on the evolution of adhesive capacities of a fish pathogen". In: *Journal of Structural Biology* 201.2 (Feb. 2018), pp. 171–183. DOI: 10.1016/j.jsb.2017.08.008.

[48] P. E. Chen, C. Cook, A. C. Stewart, N. Nagarajan, D. D. Sommer, M. Pop, B. Thomason, M. Thomason, S. Lentz, N. Nolan, S. Sozhamannan, A. Sulakvelidze, A. Mateczun, L. Du, M. E. Zwick, and T. D. Read. "Genomic characterization of the Yersinia genus". In: *Genome Biology* 11.1 (2010), R1. DOI: 10.1186/gb-2010-11-1-r1.

[49] L. Coquet, P. Cosette, G.-A. Junter, E. Beucher, J.-M. Saiter, and T. Jouenne. "Adhesion of Yersinia ruckeri to fish farm materials: influence of cell and material surface properties". In: *Colloids and Surfaces B: Biointerfaces* 26.4 (Dec. 2002), pp. 373–378. DOI: 10.1016/s0927-7765(02)00023-1.

[50] E. Tobback, A. Decostere, K. Hermans, J. Ryckaert, L. Duchateau, F. Haesebrouck, and K. Chiers. "Route of entry and tissue distribution of Yersinia ruckeri in experimentally infected rainbow trout Oncorhynchus mykiss". In: *Diseases of Aquatic Organisms* 84 (Apr. 2009), pp. 219–228. DOI: 10.3354/dao02057.

[51] E. Tobback, K. Hermans, A. Decostere, W. V. den Broeck, F. Haesebrouck, and K. Chiers. "Interactions of virulent and avirulent Yersinia ruckeri strains with isolated gill arches and intestinal explants of rainbow trout Oncorhynchus mykiss". In: *Diseases of Aquatic Organisms* 90.3 (July 2010), pp. 175–179. DOI: 10.3354/dao02230.

[52] B. L. Haines-menges, W. B. Whitaker, J. Lubin, and E. F. Boyd. "Host Sialic Acids: A Delicacy for the Pathogen with Discerning Taste". In: *Metabolism and Bacterial*

Pathogenesis. American Society of Microbiology, Jan. 2015, pp. 321–342. DOI: 10.1128/microbiolspec.mbp-0005-2014.

[53] S. Vahabi, B. N. Salman, and A. Javanmard. "Atomic force microscopy application in biological research: a review study.(Report)". English. In: *Iranian Journal of Medical Sciences* 38.2 (2013), p. 76. ISSN: 0253-0716.

[54] P. Eaton. *Atomic force microscopy*. eng. Oxford, 2010.

[55] K.-C. Chang, Y.-W. Chiang, C.-H. Yang, and J.-W. Liou. "Atomic force microscopy in biology and biomedicine". In: *Tzu Chi Medical Journal* 24.4 (Dec. 2012), pp. 162–169. DOI: 10.1016/j.tcmj.2012.08.002.

[56] M. R. Ragazzon, J. T. Gravdahl, and M. Vagia. "Viscoelastic properties of cells: Modeling and identification by atomic force microscopy". In: *Mechatronics* 50 (Apr. 2018), pp. 271–281. DOI: 10.1016/j.mechatronics.2017.09.011.

[57] V. J. Morris. *Atomic force microscopy for biologists*. eng. London, 2010.

[58] H. .-.-J. Butt and M. Jaschke. "Calculation of thermal noise in atomic force microscopy". eng. In: *Nanotechnology* 6.1 (1995), pp. 1–7. ISSN: 0957-4484.

[59] Y. F. Dufrêne. "Sticky microbes: forces in microbial cell adhesion". In: *Trends in Microbiology* 23.6 (June 2015), pp. 376–382. DOI: 10.1016/j.tim.2015.01.011.

[60] Y. F. Dufrêne. "Atomic Force Microscopy in Microbiology: New Structural and Functional Insights into the Microbial Cell Surface". In: *mBio* 5.4 (July 2014). DOI: 10.1128/mbio.01363-14.

[61] A. Razatos, Y.-L. Ong, M. M. Sharma, and G. Georgiou. "Molecular determinants of bacterial adhesion monitored by atomic force microscopy". In: *Proceedings of the National Academy of Sciences* 95.19 (Sept. 1998), pp. 11059–11064. DOI: 10.1073/pnas.95.19.11059.

[62] L. Hofherr, J. Chodorski, C. Müller-Renno, R. Ulber, and C. Ziegler. "Comparison of Versatile Immobilization Methods for Gram-Positive Bacteria on a Silicon Cantilever". In: *physica status solidi (a)* 215.15 (Jan. 2018), p. 1700846. DOI: 10.1002/pssa.201700846.

[63] M. S. Erdal. "Bacterial adhesion to mucosal surfaces". MA thesis. Trondheim: Norwegian University of Science and Technology(NTNU), May 2019. URL: http://hdl.handle.net/11250/2621739.

[64] Å. S. Ølnes. "Use of nanobiotechnology tools to study the mechanisms underlying bacterial adhesion to mucins". MA thesis. Trondheim: Norwegian University of Science and Technology(NTNU), May 2019. URL: http://hdl.handle.net/11250/2621738.

[65] Z. Iqbal, E. P. Lai, and T. J. Avis. "Antimicrobial effect of polydopamine coating on Escherichia coli". In: *Journal of Materials Chemistry* 22.40 (2012), p. 21608. DOI: 10.1039/c2jm34825j.

[66] S. Kang and M. Elimelech. "Bioinspired Single Bacterial Cell Force Spectroscopy". In: *Langmuir* 25.17 (Sept. 2009), pp. 9656–9659. DOI: 10.1021/la902247w.

[67] H. Lee, S. M. Dellatore, W. M. Miller, and P. B. Messersmith. "Mussel-Inspired Surface Chemistry for Multifunctional Coatings". In: *Science* 318.5849 (Oct. 2007), pp. 426–430. DOI: 10.1126/science.1147241.

[68] B. W. Peterson, P. K. Sharma, H. C. van der Mei, and H. J. Busscher. "Bacterial Cell Surface Damage Due to Centrifugal Compaction". In: *Applied and Environmental Microbiology* 78.1 (Oct. 2011), pp. 120–125. DOI: 10.1128/aem.06780-11.

[69] R. S. Pembrey, K. C. Marshall, and R. P. Schneider. "Cell Surface Analysis Techniques: What Do Cell Preparation Protocols Do to Cell Surface Properties?" In: *Applied and Environmental Microbiology* 65.7 (1999), p. 2877. ISSN: 0099-2240.

[70] F. Jutfelt, R. E. Olsen, J. Glette, E. Ringo, and K. Sundell. "Translocation of viable Aeromonas salmonicida across the intestine of rainbow trout, Oncorhynchus mykiss (Walbaum)". In: *Journal of Fish Diseases* 29.5 (May 2006), pp. 255–262. DOI: 10.1111/j.1365-2761.2006.00715.x.

[71] F. Jutfelt, H. Sundh, J. Glette, L. Mellander, B. T. Björnsson, and K. Sundell. "The involvement of Aeromonas salmonicida virulence factors in bacterial translocation across the rainbow trout, Oncorhynchus mykiss (Walbaum), intestine". In: *Journal of Fish Diseases* 31.2 (Jan. 2008), pp. 141–151. DOI: 10.1111/j.1365-2761.2007.00879.x.

[72] A. Viljoen, J. Mignolet, F. Viela, M. Mathelié-Guinlet, and Y. F. Dufrêne. "How Microbes Use Force To Control Adhesion". In: *Journal of Bacteriology* 202.12 (Apr. 2020). Ed. by W. Margolin. DOI: 10.1128/jb.00125-20.

[73] M. Cohen and A. Varki. "Modulation of Glycan Recognition by Clustered Saccharide Patches". eng. In: vol. 308. Netherlands: Elsevier Science Technology, 2014, pp. 75–125. ISBN: 012800097X.

[74] P. Herman, S. El-Kirat-Chatel, A. Beaussart, J. A. Geoghegan, T. J. Foster, and Y. F. Dufrêne. "The binding force of the staphylococcal adhesin SdrG is remarkably strong". In: *Molecular Microbiology* 93.2 (June 2014), pp. 356–368. DOI: 10.1111/mmi.12663.

[75] A. Beaussart, S. El-Kirat-Chatel, P. Herman, D. Alsteens, J. Mahillon, P. Hols, and Y. Dufrêne. "Single-Cell Force Spectroscopy of Probiotic Bacteria". In: *Biophysical Journal* 104.9 (May 2013), pp. 1886–1892. DOI: 10.1016/j.bpj.2013.03.046.

[76] D. Le, Y. Guérardel, P. Loubière, M. Mercier-Bonin, and E. Dague. "Measuring Kinetic Dissociation/Association Constants Between Lactococcus lactis Bacteria and Mucins Using Living Cell Probes". In: *Biophysical Journal* 101.11 (Dec. 2011), pp. 2843–2853. DOI: 10.1016/j.bpj.2011.10.034.

[77] M. Sletmoen, T. K. Dam, T. A. Gerken, B. T. Stokke, and C. F. Brewer. "Single-molecule pair studies of the interactions of the α-GalNAc (Tn-antigen) form of porcine submaxillary mucin with soybean agglutinin". In: *Biopolymers* 91.9 (Sept. 2009), pp. 719–728. DOI: 10.1002/bip.21213.

[78] P. Tripathi, A. Beaussart, D. Alsteens, V. Dupres, I. Claes, I. von Ossowski, W. M. de Vos, A. Palva, S. Lebeer, J. Vanderleyden, and Y. F. Dufrêne. "Adhesion and Nanomechanics of Pili from the Probiotic Lactobacillus rhamnosus GG". In: *ACS Nano* 7.4 (Mar. 2013), pp. 3685–3697. DOI: 10.1021/nn400705u.

[79] K. E. Haugstad, T. A. Gerken, B. T. Stokke, T. K. Dam, C. F. Brewer, and M. Sletmoen. "Enhanced Self-Association of Mucins Possessing the T and Tn Carbohydrate Cancer Antigens at the Single-Molecule Level". In: *Biomacromolecules* 13.5 (Apr. 2012), pp. 1400–1409. DOI: 10.1021/bm300135h.

[80] Y. Liu, P. A. Pinzón-Arango, A. M. Gallardo-Moreno, and T. A. Camesano. "Direct adhesion force measurements between E. coli and human uroepithelial cells in cranberry juice cocktail". In: *Molecular Nutrition & Food Research* 54.12 (Dec. 2010), pp. 1744–1752. DOI: 10.1002/mnfr.200900535.

[81] B. Austin. "The Bacterial Microflora of Fish, Revised". In: *The Scientific World JOURNAL* 6 (2006), pp. 931–945. DOI: 10.1100/tsw.2006.181.

[82] Y. S. Svendsen and J. Bøgwald. "Influence of artificial wound and non-intact mucus layer on mortality of Atlantic salmon (Salmo salar L.) following a bath challenge with *Vibrio anguillarum* and *Aeromonas salmonicida*". In: *Fish & Shellfish Immunology* 7.5 (1997), pp. 317–325.

Salmon gnotobiotic media

Contents of the salmon gnotobiotic media (SGM). The media was prepared in pre-autoclaved 1 L glass bottles and autoclaved after it was mixed together.

Table A.1: Names and amounts of the different compounds in salmon gnotobiotic medium (SGM).

Component	Amount (mL)
MgSO4	10
KCl	10
NaHCO3	10
CaSO4	200
MQ H20	770

Cultivation of Atlantic salmon fry

The atlantic salmon eggs were received 1 week before expected hatching. The embryos were transferred to large Petri dishes (140 mm diameter), 100 per dish. Approximately 75 mL SGM was transferred to every dish allowing the media to cover the embryos. The embryos were incubated in the dark at 7°C for 24 hours to acclimatize.

Each Petri dish was chosen to produce either GF, CVR or CVZ. CVR were transferred from Petri dishes to sterile conical vials. These fish fry were not treated and were kept with its original bacterial content throughout the yolk-sac stage.

GF and CVZ were sterilized before hatching. SGM were removed from the embryos and 100 mL of an antibiotic cocktail was added. The plates were gently swirled to mix the embryos with the solution. The eggs were incubated in the dark at 7°C for another 24 hours. The next day the eggs were sterilized with buffodine solution. This process was executed in a laminar flow cabinet and all the equipment involved were UV-radiated before use. The buffodine solution was prepared with SGM to create a solution of 100 mg/L available iodine. Approximately 15 healthy embryos were transferred with a pair of plastic forceps to an empty conical vial. The disinfecting solution was added to the embryos and incubated for 30 minutes. Following incubation, the buffodine solution was removed and the eggs were rinsed with SGM four times before it was transferred to a 500 mL tissue flask containing 100 mL sterile SGM.

The fish were stored in the dark at 7°C. Water changes were executed for each type of fish three times a week (monday, wednesday and friday). The CVZ had bacteria reintroduced from the hatching water one week post hatching.

AFM probes

C.1 Properties of the PNP-TR-TL cantilever

List of the properties of the PNP-TR-TL tipless cantilever used in experiments with the AFM.

	Cantilever 1	Cantilever 2
Shape:	Triangle	Triangle
Force Constant:	0.32 N/m	0.08 N/m
Resonance Frequency:	67 kHz	17 kHz
Length:	100 µm	200 µm
Width:	13.5 µm	28 µm
Thickness:	500 nm	500 nm

Figure C.1: Properties of the PNP-TR-TL cantilever (NanoAndMore GmbH)

C.2 Negative control of AFM probe without added bacteria

A probe was functionalized with PDA for 45 minutes and then stained with live/dead, without addition of bacteria. This was done to ensure that emission of green and red light would not be observed unless bacteria was present on the probe. The green and red light shown on this probe is very weak and does not show any signs of staining. This shows that without bacteria on the tip, no fluorescent light will be emitted.

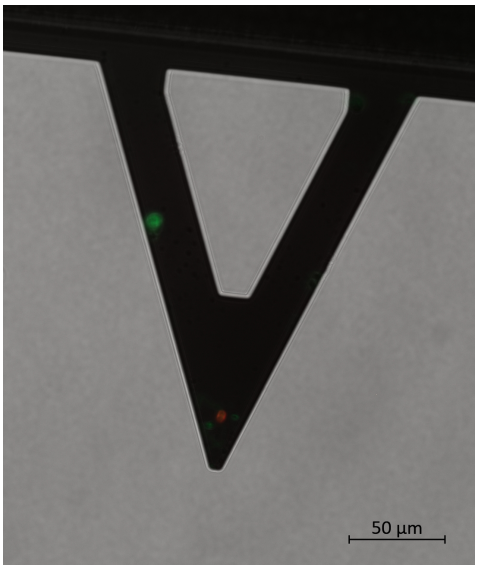

Figure C.2: Probe imaged with live/dead assay, without addition of bacteria. The probe has been treated with PDA for 45 minutes and then stained with live/dead stain.

Modifications to frequencies of deadhesion work

To portray the total deadhesion work, combined by the three replicates, modifications were made to the frequencies of some replicates. This was executed to better portray the full extent of the interactions and avoid that some interactions become more predominant than others. The frequencies from each replicate were multiplied with a specific factor, shown in table D.1 for gut mucins and table D.2 for skin mucins. After multiplying the frequencies with their factor, the three replicates for each type were added together and divided with a fitting number to yield a total percentage of 100.

Table D.1: Factors multiplied with the frequencies of the parallels A, B and C for each bacteria to mucins (treated with neuraminidase (+), untreated (-)). These factors were used with results for gut mucins

	A	B	C
A. Salmonicida (-)	1	1	1
A. Salmonicida (+)	0.5	1	0.2
Y. Ruckeri (-)	0.8	0.5	1
Y. Ruckeri (+)	0.1	0.8	0.4

Table D.2: Factors multiplied with the frequencies of the parallels A, B and C for each bacteria to mucins (treated with neuraminidase (+), untreated (-)). These factors were used with results for skin mucins

	A	B	C
A. Salmonicida (-)	1	1	0.4
A. Salmonicida (+)	0.5	1	0.2
Y. Ruckeri (-)	1	1	0.6
Y. Ruckeri (+)	0.1	1	1

Johanna Tonstad

Adhesion of common salmonid pathogens to Atlantic salmon mucins

NTNU
Norwegian University of
Science and Technology